

# ERROR ESTIMATES FOR GALERKIN APPROXIMATIONS OF THE SERRE EQUATIONS

DIMITRIOS ANTONOPOULOS, VASSILIOS DOUGALIS, AND DIMITRIOS MITSOTAKIS

**ABSTRACT.** We consider the Serre system of equations which is a nonlinear dispersive system that models two-way propagation of long waves of not necessarily small amplitude on the surface of an ideal fluid in a channel. We discretize in space the periodic initial-value problem for the system using the standard Galerkin finite element method with smooth splines on a uniform mesh and prove an optimal-order  $L^2$ -error estimate for the resulting semidiscrete approximation. Using the fourth-order accurate, explicit, ‘classical’ Runge-Kutta scheme for time stepping we construct a highly accurate fully discrete scheme in order to approximate solutions of the system, in particular solitary-wave solutions, and study numerically phenomena such as the resolution of general initial profiles into sequences of solitary waves, and overtaking collisions of pairs of solitary waves propagating in the same direction with different speeds.

## 1. INTRODUCTION

In this paper we will analyze standard Galerkin-finite element approximations to the periodic initial-value problem for the system of *Serre equations*. The system consists of two pde’s, approximates the two-dimensional Euler equations of water-wave theory, and models two-way propagation of long waves on the surface of an ideal fluid in a uniform horizontal channel of finite depth  $h_0$ . Specifically, if  $\varepsilon = a/h_0$ , where  $a$  is a typical wave amplitude, and  $\sigma = h_0/\lambda$ , where  $\lambda$  is a typical wavelength, the system is valid when  $\sigma \ll 1$  and is written in nondimensional, scaled variables in the form:

$$\zeta_t + (\eta u)_x = 0, \quad (1)$$

$$u_t + \zeta_x + \varepsilon u u_x - \frac{\sigma^2}{3\eta} [\eta^3 (u_{xt} + \varepsilon u u_{xx} - \varepsilon u_x^2)]_x = 0. \quad (2)$$

Here  $x$  and  $t$  are proportional to position along the channel and time, respectively,  $\varepsilon\zeta$ , where  $\zeta = \zeta(x, t)$ , is the elevation of the free surface above a level of rest at height  $y = 0$  of the vertical axis,  $\eta = 1 + \varepsilon\zeta$ , assumed to be positive, is the water depth (as the horizontal bottom in these variables is located at  $y = -1$ ), and  $u = u(x, t)$  is the vertically averaged horizontal velocity of the fluid. (For  $\varepsilon = O(1)$  the left-hand side of (2) is an  $O(\sigma^4)$  asymptotic approximation derived from the equation of conservation of momentum in the  $x$  direction of the 2D-Euler equations; (1) is exact.)

The system (1)-(2) was first derived by Serre, [30], and subsequently rederived by Su and Gardner, [31], by Green *et al.*, and Green and Naghdi, [17], [18], (who extended it to the case of two spatial variables and variable bottom), and others. It is also known as *Green – Naghdi* or *fully nonlinear Boussinesq system*. For its formal derivation from the Euler equations and the derivation of related systems, cf. [21]; regarding its rigorous justification as an approximation of the Euler equations we refer the reader to the recent monograph by Lannes, [20], and its references.

In case one considers long waves of *small amplitude*, specifically in the *Boussinesq* regime  $\varepsilon = O(\sigma^2)$ ,  $\sigma \ll 1$ , it is straightforward to see that the Serre system becomes

$$\begin{aligned} \zeta_t + (\eta u)_x &= 0, \\ u_t + \zeta_x + \varepsilon u u_x - \frac{\sigma^2}{3} u_{xxt} &= O(\sigma^4), \end{aligned}$$

i.e. reduces (if the right-hand side of the second equation is replaced by zero), to the ‘classical’ Boussinesq system, [34], which has a linear dispersive term in contrast to the nonlinear dispersive terms present in (2).

---

2010 *Mathematics Subject Classification.* 65M60, 35Q53.

*Key words and phrases.* Surface water waves, Serre equations, error estimates, standard Galerkin finite element methods, solitary waves.

(If the dispersive terms are omitted altogether, the system reduces to the shallow water equations.) Since it is valid for  $\varepsilon = O(1)$ , the Serre system, when written in its variable-bottom topography form, has been found suitable for the description of nonlinear dispersive waves even of larger amplitude, such as water waves in the near-shore zone before they break.

The Cauchy problem for the Serre system in nondimensional variables, that we still denote by  $x, t, u$ ,  $\eta = 1 + \zeta$ , is written for  $x \in \mathbb{R}, t \geq 0$  as

$$\eta_t + (\eta u)_x = 0, \tag{3}$$

$$u_t + \eta_x + uu_x - \frac{1}{3\eta} [\eta^3 (u_{xt} + uu_{xx} - u_x^2)]_x = 0, \tag{4}$$

with given initial conditions

$$\eta(x, 0) = \eta_0(x), \quad u(x, 0) = u_0(x), \quad x \in \mathbb{R}. \tag{5}$$

In [24] Li proved that the initial-value problem (3)-(5) is well posed locally in time for  $(\eta, u) \in H^s \times H^{s+1}$ , for  $s > 3/2$ , provided  $\min_{x \in \mathbb{R}} \eta_0(x) > 0$ , and that the property  $\min_{x \in \mathbb{R}} \eta(x, t) > 0$  is preserved while the solution exists. (Here  $H^s = H^s(\mathbb{R})$ , for  $s$  real, is the subspace of  $L^2(\mathbb{R})$  consisting of (classes of) functions  $f$  for which  $\int_{-\infty}^{\infty} (1 + \xi^2)^s |\hat{f}(\xi)|^2 d\xi < \infty$ , where  $\hat{f}$  is the Fourier transform of  $f$ .) Li also provided a rigorous justification for the Serre equations as an approximation of the Euler equations. Local well-posedness of the system in 1D in its variable bottom formulation was proved in [19]. For results on the well-posedness and justification of the general 2D Green–Naghdi equations with bottom topography, we refer the reader to [20] and its references. It should be noted that local temporal existence of the Cauchy problem for the scaled equations (1)-(2) may be established in intervals of the form  $[0, T_\varepsilon]$ , where  $T_\varepsilon = O(1/\varepsilon)$ .

It is not hard to see, cf. [17], [23], that suitably smooth and decaying solutions of (3)-(5) preserve, over their temporal interval of existence, the mass  $\int_{-\infty}^{\infty} \eta dx$ , momentum  $\int_{-\infty}^{\infty} \eta u dx$ , and energy integrals. The latter invariant (Hamiltonian) is given by

$$E = \frac{1}{2} \int_{-\infty}^{\infty} [\eta u^2 + \frac{1}{3} \eta^3 u_x^2 + (\eta - 1)^2] dx. \tag{6}$$

In addition, as Serre had already noted in the second part of his paper, [30], the system (3)-(4) possesses solitary-wave solutions and a family of periodic (cnoidal) travelling wave solutions; cf. also [11] for the latter. Closed-form formulas are known for both of these families of solutions.

In recent years many papers dealing with the numerical solution of the Serre system and its enhanced dispersion and variable bottom topography variants have appeared. In these works the reader may find, among other, numerical studies of the generation, propagation, and interaction of solitary and cnoidal waves, of the interaction of waves with boundaries, and of the effects of bottom topography on the propagation of the waves. The numerical methods used include spectral schemes, cf. e.g. [25], [15], finite difference and finite volume methods, cf. e.g. the early paper [27], and [32], [7], [9], [8] and its references, [10], [15], standard Galerkin methods, cf. e.g. [29], [28], *et al.* In some of these papers the results of numerical simulations with the Serre systems have been compared with experimental data and also with numerical solutions of the Euler equations. These comparisons bear out the effectiveness of the Serre systems in approximating the Euler equations in a variety of variable-bottom-topography test problems, cf.e.g. [32],[7],[10], especially when the equations are solved with hybrid numerical techniques, wherein the advective terms of the equations are discretized by shock-capturing techniques while the dispersive terms are treated e.g. by finite differences, cf. e.g. [8], [9].

In the paper at hand we consider the periodic initial-value problem for the Serre equations (3)-(4) with periodic initial data on the spatial interval  $[0, 1]$ , assuming that it has smooth solutions over a temporal interval  $[0, T]$  that satisfy  $\min_{(x,t) \in [0,1] \times [0,T]} \eta(x, t) > 0$ .

In section 2 we discretize the problem in space by the standard Galerkin method using the smooth periodic splines of order  $r \geq 3$  (i.e. piecewise polynomials of degree  $r - 1 \geq 2$ ) on a uniform mesh of meshlength  $h$ . We compare the Galerkin semidiscrete approximation with a suitable spline quasiinterpolant, [33], and, using the high order of accuracy of the truncation error (due to cancellations resulting from periodicity and the uniform mesh), and an energy stability and convergence argument, we prove *a priori* optimal-order error estimates in  $L^2$ , i.e. of  $O(h^r)$ , for both components of the semidiscrete solution. This is the first error estimate for a numerical method for the Serre system that we are aware of. As expected, the presence of

the nonlinear dispersive terms complicates the error analysis that is now considerably more technical than in analogous proofs of convergence in the case of Boussinesq systems, [6], and the shallow water equations, [2].

In section 3 we present the results of numerical experiments that we performed in order to approximate solutions of the periodic initial-value problem for the Serre equations using mainly cubic splines in space and the fourth-order accurate, explicit, ‘classical’ Runge-Kutta scheme for time stepping. We check first that the resulting fully discrete scheme is stable under a Courant number restriction, enjoys optimal order of accuracy in various norms, and approximates to high accuracy various types of solutions of the equations including solitary-wave solutions. We then use this scheme to illustrate properties of the solitary waves. In the preliminary section 3.1 we compare by analytical and numerical means the amplitudes  $A_S$ ,  $A_{CB}$ ,  $A_{Euler}$  of the solitary waves of, respectively, the Serre equations, the CB system, and the Euler equations, corresponding to the same speed  $c > 1$ , for small values of  $c^2 - 1$ . Our study complements the analogous numerical computations of Li *et al.*, [25], and our conclusion is that always  $A_S < A_{CB}$  and that up to about  $c = 1.2$ ,  $A_S < A_{Euler} < A_{CB}$  and  $|A_{Euler} - A_S| < |A_{Euler} - A_{CB}|$ . For larger speeds the solitary waves of both long-wave models are no longer accurate approximations of the solitary wave of the Euler equations. In section 3.2 we study numerically the *resolution* of general initial profiles into sequences of solitary waves when the evolution occurs according to the Serre or the CB equations. The number of the emerging solitary waves seems to be the same for both systems and agrees with the prediction of the asymptotic analysis of [16]. However, the emerging solitary waves of the CB equations are faster and of larger amplitude than their Serre counterparts. Finally, in section 3.3 we make a careful numerical study of *overtaking collisions* of two solitary waves of the Serre equations, as the ratio of their amplitudes is varied. We observed types of interaction that are similar to the cases (a), (b), and (c) of Lax’s Lemma 2.3 in [22] for the KdV equation. In addition, for the Serre system, there is apparently another type of interaction, intermediate between Lax’s cases (a) and (b).

In this paper we denote, for integer  $k \geq 0$ , by  $H_{per}^k = H_{per}^k(0, 1)$  the usual  $L^2$ -based Sobolev spaces of periodic functions on  $[0, 1]$  and their norms by  $\|\cdot\|_k$ . We let  $C_{per}^k = C_{per}^k[0, 1]$  be the  $k$ -times continuously differentiable 1-periodic functions. The inner product on  $L^2 = L^2(0, 1)$  is denoted by  $(\cdot, \cdot)$  and the corresponding norm simply by  $\|\cdot\|$ . The norms on  $W_\infty^k = W_\infty^k(0, 1)$  and  $L^\infty = L^\infty(0, 1)$  are denoted by  $\|\cdot\|_{k,\infty}$  and  $\|\cdot\|_\infty$ , respectively.  $\mathbb{P}_r$  are the polynomials of degree at most  $r$ .

The paper is dedicated to Jerry Bona, long-time friend, teacher and mentor, on the occasion of his 70<sup>th</sup> birthday.

**Acknowledgement:** This work was partially supported by the programmatic agreement between Research Centers-GSRT 2015-2017 in the framework of the Hellenic Republic - Siemens agreement.

D. E. Mitsotakis was supported by the Marsden Fund administered by the Royal Society of New Zealand.

## 2. GALERKIN SEMIDISCRETIZATION

We shall analyze the Galerkin semidiscrete approximation of the periodic initial-value problem for the Serre system in the following form. Assuming that  $\eta$  is positive, we multiply the pde (4) by  $\eta$  and consider the periodic initial-value problem for the resulting system. Specifically, given  $T > 0$ , for  $t \in [0, T]$  we seek 1-periodic functions  $\eta(\cdot, t)$  and  $u(\cdot, t)$  satisfying

$$\begin{aligned} \eta_t + (\eta u)_x &= 0, \\ \eta u_t + \eta \eta_x + \eta u u_x - \frac{1}{3}[\eta^3(u_{xt} + uu_{xx} - u_x^2)]_x &= 0, & (x, t) \in [0, 1] \times [0, T], \\ \eta(x, 0) = \eta_0(x), \quad u(x, 0) = u_0(x), \quad 0 \leq x \leq 1, \end{aligned} \tag{S}$$

where  $\eta_0, u_0$  are given 1-periodic functions. For the purposes of the error estimation we shall assume that  $\eta_0$  and  $u_0$  are smooth enough with  $\min_{0 \leq x \leq 1} \eta_0(x) \geq c_0 > 0$  for some constant  $c_0$  and that (S) has a unique sufficiently smooth solution  $(\eta, u)$  which is 1-periodic in  $x$  for all  $t \in [0, T]$  and is such that  $\eta(x, t) \geq c_0$  for  $(x, t) \in [0, 1] \times [0, T]$ .

**2.1. Smooth periodic splines and the quasiinterpolant.** Let  $N$  be a positive integer and  $h = 1/N$ ,  $x_i = ih$ ,  $i = 0, 1, \dots, N$ . For integer  $r \geq 2$  consider the associated  $N$ -dimensional space of smooth 1-periodic

splines

$$S_h = \{\phi \in C_{per}^{r-2}[0, 1] : \phi|_{[x_{i-1}, x_i]} \in \mathbb{P}_{r-1}, 1 \leq i \leq N\}.$$

It is well known that  $S_h$  has the following approximation properties: Given a sufficiently smooth 1-periodic function  $v$ , there exists  $\chi \in S_h$  such that

$$\sum_{j=0}^{s-1} h^j \|v - \chi\|_j \leq Ch^s \|v\|_s, \quad 1 \leq s \leq r,$$

and

$$\sum_{j=0}^{s-1} h^j \|v - \chi\|_{j,\infty} \leq Ch^s \|v\|_{s,\infty}, \quad 1 \leq s \leq r,$$

for some constant  $C$  independent of  $h$  and  $v$ . Moreover there exists a constant  $C$  independent of  $h$  such that the inverse properties

$$\begin{aligned} \|\chi\|_\beta &\leq Ch^{-(\beta-\alpha)} \|\chi\|_\alpha, \quad 0 \leq \alpha \leq \beta \leq r-1, \\ \|\chi\|_{s,\infty} &\leq Ch^{-(s+1/2)} \|\chi\|, \quad 0 \leq s \leq r-1, \end{aligned}$$

hold for all  $\chi \in S_h$ . (In the sequel we shall denote by  $C$  generic constants independent of  $h$ .)

Thomée and Wendroff, [33], proved that there exists a basis  $\{\phi_j\}_{j=1}^N$  of  $S_h$  with  $\text{supp}(\phi_j) = O(h)$ , such that if  $v$  a sufficiently smooth 1-periodic function, the associated *quasiinterpolant*  $Q_h v = \sum_{j=1}^N v(x_j) \phi_j$  satisfies

$$\|Q_h v - v\| \leq Ch^r \|v^{(r)}\|. \quad (7)$$

In addition, it was shown in [33] that the basis  $\{\phi_j\}_{j=1}^N$  may be chosen so that the following properties hold:

(i) If  $\psi \in S_h$ , then

$$\|\psi\| \leq Ch^{-1} \max_{1 \leq i \leq N} |(\psi, \phi_i)|. \quad (8)$$

(It follows from (8) that if  $\psi \in S_h$ ,  $f \in L^2$  are such that

$$(\psi, \phi_i) = (f, \phi_i) + O(h^\alpha), \quad \text{for } 1 \leq i \leq N,$$

i.e. if  $|(\psi - P_h f, \phi_i)| \leq Ch^\alpha$ ,  $1 \leq i \leq N$ , where  $P_h$  is the  $L^2$ -projection operator on  $S_h$ , then  $\|\psi\| \leq \|\psi - P_h f\| + \|P_h f\| \leq Ch^{\alpha-1} + \|f\|$ .)

(ii) Let  $w$  be a sufficiently smooth 1-periodic function and  $\nu, \kappa$  integers such that  $0 \leq \nu, \kappa \leq r-1$ . Then

$$((Q_h w)^{(\nu)}, \phi_i^{(\kappa)}) = (-1)^\kappa h w^{(\nu+\kappa)}(x_i) + O(h^{2r+j-\nu-\kappa}), \quad 1 \leq i \leq N, \quad (9)$$

where  $j = 1$  if  $\nu + \kappa$  is even and  $j = 2$  if  $\nu + \kappa$  is odd.

(iii) Let  $f, g$  be sufficiently smooth 1-periodic functions and  $\nu$  and  $\kappa$  as in (ii) above. Let

$$\beta_i = (f(Q_h g)^{(\nu)}, \phi_i^{(\kappa)}) - (-1)^\kappa (Q_h [(fg^{(\nu)})^{(\kappa)}], \phi_i), \quad 1 \leq i \leq N.$$

Then

$$\max_{1 \leq i \leq N} |\beta_i| = O(h^{2r+j-\nu-\kappa}), \quad (10)$$

where  $j$  as in (ii).

It is straightforward to see that the following result also holds for the quasiinterpolant:

**Lemma 2.1.** *Let  $r \geq 3$ ,  $v \in H_{per}^r(0, 1) \cap W_\infty^r(0, 1)$  and put  $V = Q_h v$ . Then*

$$\|V - v\|_j \leq Ch^{r-j} \|v\|_r, \quad j = 0, 1, 2, \quad (11)$$

$$\|V - v\|_{j,\infty} \leq Ch^{r-j-1/2} \|v\|_{r,\infty}, \quad j = 0, 1, 2, \quad (12)$$

$$\|V\|_j \leq C, \quad \text{and} \quad \|V\|_{j,\infty} \leq C, \quad j = 0, 1, 2. \quad (13)$$

If in addition  $\min_{0 \leq x \leq 1} v(x) \geq c_0 > 0$ , then there exists  $h_0$  such that

$$\min_{0 \leq x \leq 1} V(x) \geq c_0/2, \quad \text{for } h \leq h_0. \quad (14)$$

*Proof.* The estimates (11), (12) follow, as was remarked in [13], from the approximation and inverse properties of  $S_h$  and (7), and imply the bounds in (13). To prove (14) note that by (12)

$$V(x) = (V(x) - v(x)) + v(x) \geq -Ch^{r-1/2}\|v\|_{r,\infty} + c_0 \geq \frac{c_0}{2},$$

for  $h \leq h_0$ , with  $h_0$  such that  $Ch_0^{r-1/2}\|v\|_{r,\infty} \leq c_0/2$ .  $\square$

**2.2. Consistency of the semidiscrete approximation.** The standard Galerkin semidiscretization of (S) is defined as follows. We seek  $(\eta_h, u_h) : [0, T] \rightarrow S_h$ , satisfying for  $t \in [0, T]$  the equations

$$\begin{aligned} (\eta_{ht}, \phi) + ((\eta_h u_h)_x, \phi) &= 0, \quad \forall \phi \in S_h, \\ (\eta_h u_{ht}, \chi) + \frac{1}{3}(\eta_h^3 u_{htx}, \chi') + (\eta_h \eta_{hx}, \chi) + (\eta_h u_h u_{hx}, \chi) \\ &+ \frac{1}{3}(\eta_h^3 (u_h u_{hxx} - u_{hx}^2), \chi') = 0, \quad \forall \chi \in S_h, \end{aligned} \quad (15)$$

with initial conditions

$$\eta_h(0) = Q_h \eta_0, \quad u_h(0) = Q_h u_0. \quad (16)$$

We first establish the consistency of this semidiscretization to the p.d.e. system in (S) by proving an optimal-order  $L^2$  estimate of a suitable truncation error of (15).

**Proposition 2.1.** *Let  $(\eta, u)$  be the solution of (S) and let  $\eta, u$  be sufficiently smooth, 1-periodic in  $x$ . Let  $r \geq 3$ ,  $H = Q_h \eta$ ,  $U = Q_h u$ , and define  $\psi, \delta : [0, T] \rightarrow S_h$  by the equations*

$$\begin{aligned} (H_t, \phi) + ((HU)_x, \phi) &= (\psi, \phi), \quad \forall \phi \in S_h, \\ (HU_t, \chi) + \frac{1}{3}(H^3 U_{tx}, \chi') + (HH_x, \chi) + (HUU_x, \chi) \\ &+ \frac{1}{3}(H^3(UU_{xx} - U_x^2), \chi') = A(\delta, \chi), \quad \forall \chi \in S_h, \end{aligned} \quad (17)$$

where  $A(v, w) = (v, w) + (v', w')$  denotes the  $H^1$  inner product. Then, there exists a constant  $C$  independent of  $h$ , such that

$$\max_{0 \leq t \leq T} (\|\psi(t)\| + \|\delta(t)\|_1) \leq Ch^r. \quad (18)$$

*Proof.* Let  $\rho = Q_h \eta - \eta = H - \eta$  and  $\sigma = Q_h u - u = U - u$ . From the first pde in (S) and from (17) we obtain

$$(\psi, \phi) = (\rho_t, \phi) + ((HU)_x - (\eta u)_x, \phi), \quad \forall \phi \in S_h.$$

Since

$$(HU - \eta u)_x = ((\rho + \eta)(\sigma + u))_x - (\eta u)_x = (\rho\sigma)_x + (\eta\sigma)_x + (u\rho)_x,$$

it follows that

$$(\psi, \phi) = (\rho_t, \phi) + ((\rho\sigma)_x, \phi) + (\eta_x \sigma + u_x \rho, \phi) + (\tilde{\psi}, \phi), \quad \forall \phi \in S_h, \quad (19)$$

where  $\tilde{\psi} : [0, T] \rightarrow S_h$  is given by

$$(\tilde{\psi}, \phi) = (\eta\sigma_x, \phi) + (u\rho_x, \phi), \quad \forall \phi \in S_h.$$

In order to estimate  $\tilde{\psi}$  we take into account (10) and obtain for  $1 \leq i \leq N$

$$\begin{aligned} (\tilde{\psi}, \phi_i) &= (\eta\sigma_x, \phi_i) + (u\rho_x, \phi_i) \\ &= (\eta(Q_h u)_x - \eta u_x, \phi_i) + (u(Q_h \eta)_x - u \eta_x, \phi_i) \\ &= (Q_h(\eta u_x) - \eta u_x, \phi_i) + (Q_h(u \eta_x) - u \eta_x, \phi_i) + \gamma_i, \end{aligned}$$

where  $\max_{1 \leq i \leq N} |\gamma_i| \leq Ch^{2r+1}$ . Therefore, using the remark following (8) and (7) we conclude that

$$\|\tilde{\psi}\| \leq Ch^r. \quad (20)$$

Taking now  $\phi = \psi$  in (19), by (11), (20) we obtain

$$\|\psi\| \leq Ch^r. \quad (21)$$

Proving an analogous estimate for  $\delta$  is more complicated due to the presence of the nonlinear dispersive terms. From the second pde in (S) and (17) we see that

$$\begin{aligned} A(\delta, \chi) &= (HU_t - \eta u_t, \chi) + \frac{1}{3}(H^3 U_{tx} - \eta^3 u_{tx}, \chi') + (HH_x - \eta \eta_x, \chi) \\ &\quad + (HUU_x - \eta uu_x, \chi) + \frac{1}{3}(H^3 UU_{xx} - \eta^3 uu_{xx}, \chi') \\ &\quad - \frac{1}{3}(H^3 U_x^2 - \eta^3 u_x^2, \chi'), \quad \forall \chi \in S_h. \end{aligned} \quad (22)$$

For the first term in the right-hand side of (22) we have

$$HU_t - \eta u_t = (\rho + \eta)(\sigma_t + u_t) - \eta u_t = H\sigma_t + u_t \rho,$$

and by (7) and (13) we get

$$\|HU_t - \eta u_t\| = \|H\sigma_t + u_t \rho\| \leq Ch^r. \quad (23)$$

To treat the second term in the right-hand side of (22) we write

$$\begin{aligned} H^3 U_{tx} - \eta^3 u_{tx} &= (\rho + \eta)^3 (\sigma_{tx} + u_{tx}) - \eta^3 u_{tx} \\ &= U_{tx} \rho^3 + 3\eta U_{tx} \rho^2 + 3\eta^2 \rho \sigma_{tx} + 3\eta^2 u_{tx} \rho + \eta^3 \sigma_{tx}, \end{aligned}$$

i.e.

$$\begin{aligned} \frac{1}{3}(H^3 U_{tx} - \eta^3 u_{tx}) &= v_1 + \tilde{v}_1, \\ v_1 &= \frac{1}{3}U_{tx} \rho^3 + \eta U_{tx} \rho^2 + \eta^2 \rho \sigma_{tx}, \quad \tilde{v}_1 = \eta^2 u_{tx} \rho + \frac{1}{3}\eta^3 \sigma_{tx}, \end{aligned} \quad (24)$$

Using (13), (12), and (11) we see that

$$\begin{aligned} \|v_1\| &\leq C(\|\rho^3\| + \|\rho^2\| + \|\rho \sigma_{tx}\|) \\ &\leq C(\|\rho\|_\infty^2 \|\rho\| + \|\rho\|_\infty \|\rho\| + \|\rho\|_\infty \|\sigma_{tx}\|) \leq Ch^{2r-3/2}, \end{aligned}$$

from which it follows that

$$\|v_1\| \leq Ch^r. \quad (25)$$

For the third term we have

$$HH_x - \eta \eta_x = (\rho + \eta)(\rho_x + \eta_x) - \eta \eta_x = \rho \rho_x + \eta_x \rho + \eta \rho_x,$$

i.e.

$$\begin{aligned} HH_x - \eta \eta_x &= v_2 + \tilde{v}_2, \\ v_2 &= \rho \rho_x + \eta_x \rho, \quad \tilde{v}_2 = \eta \rho_x, \end{aligned} \quad (26)$$

while for the fourth term we write

$$\begin{aligned} HUU_x - \eta uu_x &= (\rho + \eta)(\sigma + u)(\sigma_x + u_x) - \eta uu_x \\ &= (\rho + \eta)(\sigma \sigma_x + (u\sigma)_x + uu_x) - \eta uu_x \\ &= H\sigma \sigma_x + \rho(u\sigma)_x + uu_x \rho + \eta u_x \sigma + \eta u \sigma_x, \end{aligned}$$

or

$$\begin{aligned} HUU_x - \eta uu_x &= v_3 + \tilde{v}_3, \\ v_3 &= H\sigma \sigma_x + \rho(u\sigma)_x + uu_x \rho + \eta u_x \sigma, \quad \tilde{v}_3 = \eta u \sigma_x, \end{aligned} \quad (27)$$

Using again (11)-(13) we see, as in the estimation of  $v_1$  that

$$\|v_2\| + \|v_3\| \leq Ch^r. \quad (28)$$

For the fifth term in the right-hand side of (22) we write

$$\begin{aligned} H^3 UU_{xx} - \eta^3 uu_{xx} &= (\rho + \eta)^3 (\sigma_{xx} + u_{xx}) - \eta^3 uu_{xx} \\ &= \rho^3 UU_{xx} + 3\eta \rho^2 UU_{xx} + 3\eta^2 \rho \sigma \sigma_{xx} + 3\eta^2 \rho (\sigma u_{xx} + u \sigma_{xx}) \\ &\quad + 3\eta^2 \rho uu_{xx} + \eta^3 \sigma \sigma_{xx} + \eta^3 \sigma u_{xx} + \eta^3 u \sigma_{xx}, \end{aligned}$$

i.e.

$$\begin{aligned}
\frac{1}{3}(H^3UU_{xx} - \eta^3uu_{xx}) &= v_4 + \tilde{v}_4, \\
v_4 &= \frac{1}{3}UU_{xx}\rho^3 + \eta UU_{xx}\rho^2 + \eta^2\rho\sigma\sigma_{xx} + \eta^2(u_{xx}\rho\sigma + u\rho\sigma_{xx}) + \frac{1}{3}\eta^3\sigma\sigma_{xx} \\
\tilde{v}_4 &= \eta^2uu_{xx}\rho + \frac{1}{3}\eta^3u_{xx}\sigma + \frac{1}{3}\eta^3u\sigma_{xx}.
\end{aligned} \tag{29}$$

Hence, from (11)-(13)

$$\begin{aligned}
\|v_4\| &\leq C(\|\rho\|_\infty^2\|\rho\| + \|\rho\|_\infty\|\rho\| + \|\rho\|_\infty\|\sigma\|_\infty\|\sigma_{xx}\| \\
&\quad + \|\rho\|_\infty\|\sigma\| + \|\rho\|_\infty\|\sigma_{xx}\| + \|\sigma\|_\infty\|\sigma_{xx}\|) \leq Ch^{2r-5/2}.
\end{aligned}$$

Therefore, since  $r \geq 3$ ,

$$\|v_4\| \leq Ch^r. \tag{30}$$

Finally, for the last term in the right-hand side of (22) we have

$$\begin{aligned}
H^3U_x^2 - \eta^3u_x^2 &= (\rho + \eta)^3(\sigma_x + u_x)^2 - \eta^3u_x^2 \\
&= \rho^3U_x^2 + 3\eta\rho^2U_x^2 + 3\eta^2\rho(\sigma_x^2 + 2u_x\sigma_x + u_x^2) + \eta^3(\sigma_x^2 + 2u_x\sigma_x),
\end{aligned}$$

i.e.

$$\begin{aligned}
\frac{1}{3}(H^3U_x^2 - \eta^3u_x^2) &= v_5 + \tilde{v}_5, \\
v_5 &= \frac{1}{3}\rho^3U_x^2 + \eta\rho^2U_x^2 + \eta^2\rho\sigma_x^2 + 2\eta^2\rho u_x\sigma_x + \frac{1}{3}\eta^3\sigma_x^2, \\
\tilde{v}_5 &= \eta^2u_x^2\rho + \frac{2}{3}\eta^3u_x\sigma_x.
\end{aligned} \tag{31}$$

From (11)-(13) we have as before

$$\begin{aligned}
\|v_5\| &\leq C(\|\rho\|_\infty^2\|\rho\| + \|\rho\|_\infty\|\rho\| + \|\rho\|_\infty\|\sigma_x\|_\infty\|\sigma_x\| \\
&\quad + \|\rho\|_\infty\|\sigma_x\| + \|\sigma_x\|_\infty\|\sigma_x\|) \leq Ch^{2r-5/2},
\end{aligned}$$

which gives, since  $r \geq 3$ ,

$$\|v_5\| \leq Ch^r. \tag{32}$$

Hence, from (22), (24), (26), (27), (29), and (30) we have for  $\chi \in S_h$

$$A(\delta, \chi) = (H\sigma_t + u_t\rho, \chi) + (v_1, \chi') + (v_2 + v_3, \chi) + (v_4 - v_5, \chi') + (\tilde{\delta}, \chi), \tag{33}$$

where we have defined  $\tilde{\delta} : [0, T] \rightarrow S_h$  by the equation

$$(\tilde{\delta}, \chi) = (\tilde{v}_1, \chi') + (\tilde{v}_2, \chi) + (\tilde{v}_3, \chi) + (\tilde{v}_4, \chi') - (\tilde{v}_5, \chi'), \quad \chi \in S_h.$$

Using the definitions of  $\tilde{v}_i$ ,  $1 \leq i \leq 5$ , from (24), (26), (27), (29), and (31), we obtain for  $\chi \in S_h$

$$\begin{aligned}
(\tilde{\delta}, \chi) &= (\eta^2u_{tx}\rho, \chi') + \frac{1}{3}(\eta^3\sigma_{tx}, \chi') + (\eta\rho_x, \chi) + (\eta u\sigma_x, \chi) + (\eta^2uu_{xx}\rho, \chi') \\
&\quad + \frac{1}{3}(\eta^3u_{xx}\sigma, \chi') + \frac{1}{3}(\eta^3u\sigma_{xx}, \chi') - (\eta^2u_x^2\rho, \chi') - \frac{2}{3}(\eta^3u_x\sigma_x, \chi').
\end{aligned} \tag{34}$$

The term  $(\tilde{\delta}, \chi)$  consists, like  $(\tilde{\psi}, \phi)$ , of  $L^2$  inner products of  $\rho$ ,  $\sigma$ ,  $\sigma_t$  and their spatial derivatives with  $\chi$  or  $\chi'$  and with smooth periodic functions as weights. To treat these terms we invoke again the cancellation

property (10) of the quasiinterpolant and write for  $1 \leq i \leq N$

$$\begin{aligned}
(\tilde{\delta}, \phi_i) &= (\eta^2 u_{tx} Q_h \eta, \phi'_i) - (\eta^3 u_{tx}, \phi'_i) + \frac{1}{3}(\eta^3 (Q_h u_t)_x, \phi'_i) - \frac{1}{3}(\eta^3 u_{tx}, \phi'_i) \\
&\quad + (\eta (Q_h \eta)_x, \phi_i) - (\eta \eta_x, \phi_i) + (\eta u (Q_h u)_x, \phi_i) - (\eta u u_x, \phi_i) \\
&\quad + (\eta^2 u u_{xx} Q_h \eta, \phi'_i) - (\eta^3 u u_{xx}, \phi'_i) + \frac{1}{3}(\eta^3 u_{xx} Q_h u, \phi'_i) - \frac{1}{3}(\eta^3 u_{xx} u, \phi'_i) \\
&\quad + \frac{1}{3}(\eta^3 u (Q_h u)_{xx}, \phi'_i) - \frac{1}{3}(\eta^3 u u_{xx}, \phi'_i) - (\eta^2 u_x^2 Q_h \eta, \phi'_i) + (\eta^3 u_x^2, \phi'_i) \\
&\quad - \frac{2}{3}(\eta^3 u_x (Q_h u)_x, \phi'_i) + \frac{2}{3}(\eta^3 u_x^2, \phi'_i) \\
&= -(Q_h [(\eta^3 u_{tx})_x] - (\eta^3 u_{tx})_x, \phi_i) + \gamma_i^{(1)} \\
&\quad - \frac{1}{3}(Q_h [(\eta^3 u_{tx})_x] - (\eta^3 u_{tx})_x, \phi_i) + \gamma_i^{(2)} + (Q_h (\eta \eta_x) - \eta \eta_x, \phi_i) + \gamma_i^{(3)} \\
&\quad + (Q_h (\eta u u_x) - \eta u u_x, \phi_i) + \gamma_i^{(4)} - (Q_h [(\eta^3 u u_{xx})_x] - (\eta^3 u u_{xx})_x, \phi_i) + \gamma_i^{(5)} \\
&\quad - \frac{1}{3}(Q_h [(\eta^3 u u_{xx})_x] - (\eta^3 u u_{xx})_x, \phi_i) + \gamma_i^{(6)} \\
&\quad - \frac{1}{3}(Q_h [(\eta^3 u u_{xx})_x] - (\eta^3 u u_{xx})_x, \phi_i) + \gamma_i^{(7)} \\
&\quad + (Q_h [(\eta^3 u_x^2)_x] - (\eta^3 u_x^2)_x, \phi_i) + \gamma_i^{(8)} \\
&\quad + \frac{2}{3}(Q_h [(\eta^3 u_x^2)_x] - (\eta^3 u_x^2)_x, \phi_i) + \gamma_i^{(9)},
\end{aligned}$$

where  $\max_{1 \leq i \leq N} (|\gamma_i^{(1)}| + |\gamma_i^{(3)}| + |\gamma_i^{(4)}| + |\gamma_i^{(5)}| + |\gamma_i^{(6)}| + |\gamma_i^{(8)}|) \leq Ch^{2r+1}$ , while  $\max_{1 \leq i \leq N} (|\gamma_i^{(2)}| + |\gamma_i^{(7)}| + |\gamma_i^{(9)}|) \leq Ch^{2r-1}$ . Therefore, by the remark following (8) and by (7) we conclude

$$\|\tilde{\delta}\| \leq C(h^{2r-2} + h^r) \leq Ch^r. \quad (35)$$

Putting now  $\chi = \delta$  in (33) and using (23), (25), (28), (30), (32), and (35) we obtain finally

$$\|\delta\|_1 \leq Ch^r, \quad (36)$$

which together with (21) gives the desired estimate (18).  $\square$

**2.3. Error estimate.** We now prove using an energy technique an optimal-order  $L^2$  estimate for the error of the semidiscrete approximation defined by the initial-value problem (15)-(16).

**Theorem 2.1.** *Suppose that the solution  $(\eta, u)$  of (S) is sufficiently smooth and satisfies  $\min_{0 \leq x \leq 1} \eta(x, t) \geq c_0$  for  $t \in [0, T]$  for some positive constant  $c_0$ . Suppose that  $r \geq 3$  and that  $h$  is sufficiently small. Then, there is a unique solution  $(\eta_h, u_h)$  of (15)-(16) on  $[0, T]$ , which satisfies*

$$\max_{0 \leq t \leq T} (\|\eta(t) - \eta_h(t)\| + \|u(t) - u_h(t)\|) \leq Ch^r. \quad (37)$$

*Proof.* Clearly the ode initial-value-problem (15)-(16) has a unique solution locally in  $t$ . While this solution exists we let  $H = Q_h \eta$ ,  $U = Q_h u$ ,  $\theta = H - \eta_h$ , and  $\xi = U - u_h$ . Using (15) and (17) we have

$$\begin{aligned}
(\theta_t, \phi) + ((HU)_x - (\eta_h u_h)_x, \phi) &= (\psi, \phi), \quad \forall \phi \in S_h, \\
(HU_t - \eta_h u_{ht}, \chi) + \frac{1}{3}(H^3 U_{tx} - \eta_h^3 u_{htx}, \chi') + (w_1 + w_2, \chi) \\
&\quad + \frac{1}{3}(w_3 - w_4, \chi') = A(\delta, \chi), \quad \forall \chi \in S_h,
\end{aligned} \quad (38)$$

where

$$\begin{aligned}
w_1 &= HH_x - \eta_h \eta_{hx}, & w_2 &= HUU_x - \eta_h u_h u_{hx}, \\
w_3 &= H^3 UU_{xx} - \eta_h^3 u_h u_{hxx}, & w_4 &= H^3 U_x^2 - \eta_h^3 u_{hx}^2.
\end{aligned}$$

Since

$$HU - \eta_h u_h = H(U - u_h) + U(H - \eta_h) - (H - \eta_h)(U - u_h),$$

it follows that

$$HU - \eta_h u_h = H\xi + U\theta - \theta\xi, \quad (39)$$



and, consequently, from the first equation in (38)

$$(\theta_t, \phi) + ((H\xi)_x, \phi) + ((U\theta)_x, \phi) - ((\theta\xi)_x, \phi) = (\psi, \phi), \quad \forall \phi \in S_h. \quad (40)$$

From (40), putting  $\phi = \theta$  and using integration by parts, we obtain

$$\frac{1}{2} \frac{d}{dt} \|\theta\|^2 + ((H\xi)_x, \theta) + \frac{1}{2} (U_x \theta, \theta) - ((\theta\xi)_x, \theta) = (\psi, \theta). \quad (41)$$

Now, putting  $\chi = \xi$  in the second equation in (38) we see that

$$(HU_t - \eta_h u_{ht}, \xi) + \frac{1}{3} (H^3 U_{tx} - \eta_h^3 u_{htx}, \xi_x) + (w_1 + w_2, \xi) + \frac{1}{3} (w_3 - w_4, \xi_x) = A(\delta, \xi). \quad (42)$$

For the first term in the left-hand side of (42) we have

$$HU_t - \eta_h u_{ht} = H(U_t - u_{ht}) - (H - \eta_h)(U_t - u_{ht}) + U_t(H - \eta_h),$$

that is

$$HU_t - \eta_h u_{ht} = H\xi_t - \theta\xi_t + U_t\theta,$$

and therefore

$$\begin{aligned} (HU_t - \eta_h u_{ht}, \xi) &= (H\xi_t, \xi) - (\theta\xi_t, \xi) + (U_t\theta, \xi) \\ &= \frac{1}{2} \frac{d}{dt} \int_0^1 H(x, t) \xi^2(x, t) dx - \frac{1}{2} (H_t, \xi^2) \\ &\quad - \frac{1}{2} \frac{d}{dt} \int_0^1 \theta(x, t) \xi^2(x, t) dx + \frac{1}{2} (\theta_t, \xi^2) + (U_t\theta, \xi). \end{aligned} \quad (43)$$

For the second term in the left-hand side of (42) it holds that

$$\begin{aligned} H^3 U_{tx} - \eta_h^3 u_{htx} &= H^3 (U_{tx} - u_{htx}) + (H^3 - \eta_h^3) U_{tx} - (H^3 - \eta_h^3) (U_{tx} - u_{htx}) \\ &= H^3 \xi_{tx} + (H^3 - \eta_h^3) U_{tx} - (H^3 - \eta_h^3) \xi_{tx}, \end{aligned}$$

from which

$$(H^3 U_{tx} - \eta_h^3 u_{htx}, \xi_x) = (H^3 \xi_{tx}, \xi_x) + ((H^3 - \eta_h^3) U_{tx}, \xi_x) - ((H^3 - \eta_h^3) \xi_{tx}, \xi_x).$$

Hence,

$$\begin{aligned} \frac{1}{3} (H^3 U_{tx} - \eta_h^3 u_{htx}, \xi_x) &= \frac{1}{6} \frac{d}{dt} \int_0^1 H^3(x, t) \xi_x^2(x, t) dx - \frac{1}{2} (H^2 H_t, \xi_x^2) \\ &\quad + \frac{1}{3} ((H^3 - \eta_h^3) U_{tx}, \xi_x) - \frac{1}{6} \frac{d}{dt} \int_0^1 (H^3 - \eta_h^3)(x, t) \xi_x^2(x, t) dx \\ &\quad + \frac{1}{2} (H^2 H_t - \eta_h^2 \eta_{ht}, \xi_x^2). \end{aligned} \quad (44)$$

For  $w_1$  we have

$$\begin{aligned} w_1 &= HH_x - \eta_h \eta_{hx} = H(H_x - \eta_{hx}) + H_x(H - \eta_h) - (H - \eta_h)(H_x - \eta_{hx}) \\ &= (H\theta)_x - \theta\theta_x, \end{aligned}$$

i.e.

$$(w_1, \xi) = -(H\theta, \xi_x) - (\theta\theta_x, \xi). \quad (45)$$

Moreover

$$w_2 = HUU_x - \eta_h u_h u_{hx} = HU(U_x - u_{hx}) + (HU - \eta_h u_h)U_x - (HU - \eta_h u_h)(U_x - u_{hx}),$$

and in view of (39)

$$w_2 = HU\xi_x + (H\xi + U\theta - \theta\xi)U_x - (HU - \eta_h u_h)\xi_x.$$

Thus, integrating by parts,

$$\begin{aligned} (w_2, \xi) &= -\frac{1}{2} ((HU)_x, \xi^2) + (HU_x, \xi^2) + (UU_x\theta, \xi) - (U_x\theta\xi, \xi) \\ &\quad + \frac{1}{2} ((HU - \eta_h u_h)_x, \xi^2). \end{aligned} \quad (46)$$

Now, since

$$\begin{aligned} w_3 &= H^3 U U_{xx} - \eta_h^3 u_h u_{hxx} = H^3 U U_{xx} - \eta_h^3 u_h (U_{xx} - \xi_{xx}) \\ &= \eta_h^3 u_h \xi_{xx} + (H^3 U - \eta_h^3 u_h) U_{xx}, \end{aligned}$$

and since

$$H^3 U - \eta_h^3 u_h = H^3 U - \eta_h^3 (U - \xi) = (H^3 - \eta_h^3) U + \eta_h^3 \xi,$$

we get

$$w_3 = \eta_h^3 u_h \xi_{xx} + (H^3 - \eta_h^3) U U_{xx} + \eta_h^3 U_{xx} \xi,$$

and therefore

$$(w_3, \xi_x) = -\frac{1}{2}(3\eta_h^2 \eta_{hx} u_h + \eta_h^3 u_{hx}, \xi_x^2) + ((H^3 - \eta_h^3) U U_{xx}, \xi_x) + (\eta_h^3 U_{xx} \xi, \xi_x). \quad (47)$$

In addition

$$\begin{aligned} w_4 &= H^3 U_x^2 - \eta_h^3 u_{hx}^2 = H^3 U_x^2 - \eta_h^3 (U_x - \xi_x)^2 = (H^3 - \eta_h^3) U_x^2 + 2\eta_h^3 U_x \xi_x - \eta_h^3 \xi_x^2 \\ &= (H^3 - \eta_h^3) U_x^2 + \eta_h^3 U_x \xi_x + \eta_h^3 u_{hx} \xi_x. \end{aligned}$$

Hence, from this relation and (47) it follows that

$$\begin{aligned} (w_3 - w_4, \xi_x) &= ((H^3 - \eta_h^3)(U U_{xx} - U_x^2), \xi_x) - \frac{3}{2}(\eta_h^2 \eta_{hx} u_h + \eta_h^3 u_{hx}, \xi_x^2) \\ &\quad + (\eta_h^3 U_{xx} \xi, \xi_x) - (\eta_h^3 U_x, \xi_x^2). \end{aligned} \quad (48)$$

Noting that

$$((H\xi)_x, \theta) - ((\theta\xi)_x, \theta) - (H\theta, \xi_x) - (\theta\theta_x, \xi) = (H_x \xi, \theta),$$

and taking into account (45), (43), (44), (46), and (48), if we add (41) and (42) we obtain

$$\begin{aligned} &\frac{1}{2} \frac{d}{dt} \|\theta\|^2 + \frac{1}{2} \frac{d}{dt} \int_0^1 [H(x, t) \xi^2(x, t) + \frac{1}{3} H^3(x, t) \xi_x^2(x, t)] dx \\ &= \frac{1}{2} \frac{d}{dt} \int_0^1 \theta(x, t) \xi^2(x, t) dx + \frac{1}{6} \frac{d}{dt} \int_0^1 (H^3 - \eta_h^3)(x, t) \xi_x^2(x, t) dx \\ &\quad + \tilde{w}_1 + \tilde{w}_2 + \tilde{w}_3 + \tilde{w}_4, \end{aligned} \quad (49)$$

where

$$\begin{aligned} \tilde{w}_1 &= -(H_x \xi, \theta) - \frac{1}{2} (U_x \theta, \theta), \quad \tilde{w}_2 = \frac{1}{2} (H_t, \xi^2) - \frac{1}{2} (\theta_t, \xi^2) - (U_t \theta, \xi), \\ \tilde{w}_3 &= \frac{1}{2} (H^2 H_t, \xi_x^2) - \frac{1}{3} ((H^3 - \eta_h^3) U_{tx}, \xi_x) - \frac{1}{2} (H^2 H_t - \eta_h^2 \eta_{ht}, \xi_x^2), \\ \tilde{w}_4 &= -(w_2, \xi) - \frac{1}{3} (w_3 - w_4, \xi_x) + (\psi, \theta) + A(\delta, \xi). \end{aligned}$$

From (13) it follows that

$$|\tilde{w}_1| \leq C \|\theta\| \|\xi\| + C \|\theta\|^2. \quad (50)$$

Taking into account (16), (11), (12), a straightforward estimate for  $\theta_t$  that we get from (40) with  $\phi = \theta$ , and arguing by continuity, we conclude that there is a maximal time  $t_h \in (0, T]$  such that the solution of (15)-(16) exists for  $0 \leq t \leq t_h$  and satisfies

$$\max_{0 \leq s \leq t_h} (\|\theta_t(s)\|_\infty + \|\theta(s)\|_{1,\infty} + \|\xi(s)\|_{1,\infty}) \leq 1. \quad (Y)$$

Then, from (Y) and (13) it follows for  $0 \leq t \leq t_h$  that

$$|\tilde{w}_2| \leq C \|\xi\|^2 + C \|\theta\| \|\xi\|, \quad (51)$$

To derive a bound for  $\tilde{w}_3$ , note that  $H^3 - \eta_h^3 = \theta(H^2 + H\eta_h + \eta_h^2)$ , and therefore that

$$\tilde{w}_3 = -\frac{1}{3} (H^2 U_{tx} \theta, \xi_x) - \frac{1}{3} (H U_{tx} \eta_h \theta, \xi_x) - \frac{1}{3} (U_{tx} \eta_h^2 \theta, \xi_x) + \frac{1}{2} (\eta_h^2 \eta_{ht}, \xi_x^2).$$

Since  $\|\eta_h\|_{1,\infty} \leq \|\theta\|_{1,\infty} + \|H\|_{1,\infty}$ , it follows from (Y) and (13) that  $\|\eta_h\|_{1,\infty} \leq C$  for  $0 \leq t \leq t_h$ . Similarly,  $\|\eta_{ht}\|_\infty \leq C$  for  $0 \leq t \leq t_h$ . Therefore, using again (13) we conclude for  $0 \leq t \leq t_h$  that

$$|\tilde{w}_3| \leq C(\|\theta\| \|\xi_x\| + \|\xi_x\|^2). \quad (52)$$

For  $\tilde{w}_4$ , using the definitions of  $w_2, w_3, w_4$ , noting as before that (Y) implies  $\|u_h\|_{1,\infty} \leq C$  for  $0 \leq t \leq t_h$ , and using again (Y), (13), the identity  $H^3 - \eta_h^3 = \theta(H^2 + H\eta_h + \eta_h^2)$ , and (18), gives for  $0 \leq t \leq t_h$

$$|\tilde{w}_4| \leq C[\|\xi\|^2 + \|\theta\|\|\xi\| + \|\theta\|\|\xi_x\| + \|\xi_x\|^2 + \|\xi\|\|\xi_x\| + h^r(\|\theta\| + \|\xi\|_1)]. \quad (53)$$

Therefore, from (49), and taking into account (50)-(53), we obtain for  $0 \leq t \leq t_h$  that

$$\begin{aligned} \frac{1}{2} \frac{d}{dt} \|\theta(t)\|^2 + \frac{1}{2} \frac{d}{dt} \int_0^1 [H(x,t)\xi^2(x,t) + H^3(x,t)\xi_x^2(x,t)] dx &\leq \frac{1}{2} \frac{d}{dt} \int_0^1 \theta(x,t)\xi^2(x,t) dx \\ &+ \frac{1}{6} \frac{d}{dt} \int_0^1 (H^3 - \eta_h^3)(x,t)\xi_x^2(x,t) dx + C(\|\theta(t)\| + \|\xi(t)\|_1)^2 + Ch^{2r}. \end{aligned}$$

Integrating both sides of this inequality with respect to  $t$  and taking again into account (Y) and noting that  $\theta(0) = \xi(0) = 0$ , yields for  $t \leq t_h$  that

$$\begin{aligned} \frac{1}{2} \|\theta(t)\|^2 + \frac{1}{2} \int_0^1 [H(x,t)\xi^2(x,t) + \frac{1}{3}H^3(x,t)\xi_x^2(x,t)] dx \\ \leq C \int_0^t (\|\theta(s)\|^2 + \|\xi(s)\|_1^2) ds + Ch^{2r}. \end{aligned} \quad (54)$$

The left-hand side of this inequality is a sort of discrete analog of the Hamiltonian, cf. (6), appropriate for the periodic Serre system. From our hypothesis that  $\min_{0 \leq x \leq 1} \eta(x,t) \geq c_0 > 0$  for each  $t \in [0, T]$  and (14) of Lemma 2.1, we conclude from (54) that

$$\|\theta(t)\|^2 + \|\xi(t)\|_1^2 \leq C_0 \int_0^t (\|\theta(s)\|^2 + \|\xi(s)\|_1^2) ds + C_0 h^{2r},$$

holds for  $0 \leq t \leq t_h$  for a constant  $C_0$  independent of  $t_h$  and  $h$ . From this relation and Gronwall's lemma it follows that

$$\|\theta(t)\| + \|\xi(t)\|_1 \leq C_1 h^r, \quad \text{for } t \leq t_h, \quad (55)$$

for a constant  $C_1 = C_1(T)$  independent of  $t_h$  and  $h$ . This inequality and the inverse properties of  $S_h$  yield that  $\|\theta\|_{1,\infty} \leq Ch^{r-3/2}$  and  $\|\xi\|_{1,\infty} \leq Ch^{r-1/2}$  for  $t \leq t_h$ . In addition, it is straightforward to see that taking  $\phi = \theta_t$  in (40) and using (55) gives  $\|\theta_t\| \leq Ch^{r-1}$  and, therefore, that  $\|\theta_t\|_\infty \leq Ch^{r-3/2}$  for  $0 \leq t \leq t_h$ . We conclude that  $\|\theta_t\|_\infty + \|\theta\|_{1,\infty} + \|\xi\|_{1,\infty} \leq Ch^{r-3/2}$  for  $0 \leq t \leq t_h$ . This implies, provided  $h$  was taken sufficiently small, that  $t_h$  was not maximal in (Y). Hence, we may take  $t_h = T$ , and (37) follows from (55) and (11).  $\square$

**2.4. Remarks.** (i) It is straightforward to see that the error estimate (37) still holds if we take any initial condition  $\eta_h(0) \in S_h$  in (16) that satisfies  $\|\eta_h(0) - \eta_0\| \leq Ch^r$ , e.g. the  $L^2$  projection or the interpolant of  $\eta_0$  on  $S_h$ . Then (7) implies that  $\|\theta(0)\| \leq Ch^r$ , and one may easily check that (Y) is still valid for some  $t_h \in (0, T]$ , and that (54), and therefore (55), still hold. The conclusion of Theorem 2.3 follows.

(ii) The error estimate (37) is still valid if we choose as initial condition  $u_h(0)$  an 'elliptic' projection of  $u_0$  on  $S_h$  defined in terms of the bilinear form

$$B_{Serre}(\chi, \phi; \eta_0) := (\eta_0 \chi, \phi) + \frac{1}{3}(\eta_0^3 \chi', \phi'), \quad \chi, \phi \in S_h.$$

Indeed, if  $v_h \in S_h$  is the unique (since  $\eta_0 \geq c_0 > 0$ ) function in  $S_h$  for which

$$(\eta_0 v_h, \phi) + \frac{1}{3}(\eta_0^3 v_h', \phi') = (\eta_0 u_0, \phi) + \frac{1}{3}(\eta_0^3 u_0', \phi'), \quad \forall \phi \in S_h, \quad (56)$$

then

$$\|Q_h u_0 - v_h\|_1 \leq Ch^r, \quad (57)$$

i.e.  $v_h$  is superoptimally close to  $Q_h u_0$  in  $H_{per}^1$ . To see this, note that if  $\varepsilon_h = Q_h u_0 - v_h$  and  $e = Q_h u_0 - u_0$ , then

$$(\eta_0 \varepsilon_h, \phi) + \frac{1}{3}(\eta_0^3 \varepsilon_h', \phi') = (\eta_0 e, \phi) + \frac{1}{3}(\eta_0^3 e', \phi'), \quad \forall \phi \in S_h. \quad (58)$$

Define now  $\gamma \in S_h$  by the equation

$$(\gamma, \phi) = (\eta_0 e, \phi) + \frac{1}{3}(\eta_0^3 e', \phi'), \quad \forall \phi \in S_h. \quad (59)$$

Using the properties of the quasiinterpolant, and in particular (10), we have for  $1 \leq i \leq N$

$$(\eta_0 e, \phi_i) = (\eta_0 Q_h u_0 - \eta_0 u_0, \phi_i) = (Q_h(\eta_0 u_0) - \eta_0 u_0, \phi_i) + \beta_i^{(1)},$$

where  $\max_{1 \leq i \leq N} |\beta_i^{(1)}| \leq Ch^{2r+1}$ . Similarly,

$$(\eta_0^3 e', \phi_i) = -(Q_h [(\eta_0^3 u_0')'] - (\eta_0^3 u_0')', \phi_i) + \beta_i^{(2)},$$

where  $\max_{1 \leq i \leq N} |\beta_i^{(2)}| \leq Ch^{2r-1}$ . We conclude, in view of (59), (7), and the remark following (8), that

$$\|\gamma\| \leq C(h^r + h^{2r-2}) \leq Ch^r.$$

Therefore, since (58) and (59) imply

$$(\eta_0 \varepsilon_h, \phi) + \frac{1}{3}(\eta_0^3 \varepsilon_h', \phi') = (\gamma, \phi), \quad \forall \phi \in S_h,$$

putting  $\phi = \varepsilon_h$  yields  $\|\varepsilon_h\|_1 \leq C\|\gamma\| \leq Ch^r$ , i.e. that (57) is valid.

We take now  $u_h(0) = v_h$  as initial condition in (16). Note that (Y) still holds for some  $t_h \in (0, T]$ , since  $\|\xi(0)\|_1 = \|Q_h u_0 - v_h\|_1 \leq Ch^r$  and therefore  $\|\xi(0)\|_{1,\infty} \leq Ch^{r-1/2}$ . Moreover (54) and (55) still hold and the conclusion of Theorem 2.3 follows. From this and the previous remark it is clear that the usual B-spline basis may be used in the finite element computations, i.e. that there is no need of computing with the special basis  $\{\phi_i\}_{i=1}^N$ .

### 3. NUMERICAL EXPERIMENTS

In this section we present the results of some numerical experiments that we performed to approximate solutions of the periodic initial-value problem for the Serre equations using the standard Galerkin semidiscretization (15) with the spatial interval taken to be of the form  $[-L, L]$ , so that  $h = 2L/N$ . We generally used cubic splines, i.e.  $S_h$  with  $r = 4$ , and computed the initial values  $\eta_h(0)$ ,  $u_h(0)$  as the  $L^2$  projections of  $\eta_0$ ,  $u_0$  on  $S_h$ . The semidiscrete initial-value problem was discretized in time by the ‘classical’, explicit, 4<sup>th</sup>-order accurate Runge-Kutta scheme, with a uniform time step denoted by  $k$ . This fully discrete scheme was used in simulations of solutions of the Serre system in [29]. Numerical evidence from [29] and the present work, and also theoretical and numerical evidence from [4] and [3] in the case of the ‘classical’ Boussinesq system, a close relative of the Serre equations, suggests that the fully discrete method under considerations is fourth-order accurate in the temporal variable and stable under a Courant number restriction of the form  $k/h \leq r_0$ .

We checked the accuracy of the fully discrete scheme by taking as solution of the Serre system the solitary wave, [30], given by  $\eta_S(x - x_0 - ct)$ ,  $u_S(x - x_0 - ct)$ , where  $c > 1$  and

$$\begin{aligned} \eta_S(\xi) &= 1 + A_S \operatorname{sech}^2(K\xi), & u_S(\xi) &= c \left(1 - \frac{1}{\eta_S(\xi)}\right), \\ A_S &= c^2 - 1, & K &= \sqrt{\frac{3A_S}{4c^2}}. \end{aligned} \tag{60}$$

In the numerical experiments we took  $c = 1.2$  and integrated on the spatial interval  $[-150, 150]$  up to  $T = 100$ . (The solution is effectively periodic; initially the solitary wave was centered at  $x_0 = -100$  and the value of  $\eta_S$  at  $x = \pm 150$  differed from 1 by an amount smaller than the machine epsilon.) We took  $h = 2L/N = 300/N$ ,  $k = T/M$  and computed with a fixed ratio  $k/h = 0.1$  for increasing  $N$ . In the case of cubic spline space discretization the numerical convergence rates in the  $L^2$  and  $L^\infty$  norms approached four, while those in the  $H^1$  and  $H^2$  norms three and two, respectively. (The order of magnitude of the  $L^2$  errors for  $\eta$  ranged from  $10^{-6}$  for  $N = 600$  to  $10^{-10}$  for  $N = 6000$ ). The observed optimal-order  $L^2$  and  $L^\infty$  rates also suggest that there is no temporal order reduction in the scheme. It should also be noted that for this experiment the relative errors (with respect to their initial values) of two invariants of the problem, namely the energy (Hamiltonian)  $E$ , defined by the analogous to (6) formula on  $[-L, L]$ , and the momentum  $I = \int_{-L}^L \eta u dx$ , ranged, at  $T = 100$ , from  $O(10^{-7})$  for  $N = 600$  to  $O(10^{-12})$  for  $N = 6000$  in the case of  $E$ , and from  $O(10^{-8})$  for  $N = 600$  to  $O(10^{-13})$  for  $N = 3750$  for  $I$ . (The mass  $\int_{-L}^L \eta dx$  was preserved of course to machine epsilon.) We conclude that the outcome of these experiments confirms that of the analogous computations in [29].

In the case of quadratic splines the numerical convergence rates in the  $L^2$  and  $L^\infty$  norms approached three as  $N$  increased, while those corresponding to the  $H^1$  and  $H^2$  norms approached two and one, respectively, as expected. The  $L^2$  errors for  $\eta$  ranged from  $O(10^{-5})$  for  $N = 600$  to  $O(10^{-8})$  for  $N = 6000$ , while the relative errors of the invariants ranged, for the same values of  $N$ , from  $O(10^{-6})$  to  $O(10^{-10})$  for  $E$  and from  $O(10^{-7})$  to  $O(10^{-12})$  for  $I$ . It was also noted that at the spatial nodes  $x_i$  the errors of the scheme with quadratic splines appeared to be  $O(h^4)$ , i.e. superconvergent.

As noted above, the fully discrete scheme requires for stability a bound on the Courant number  $k/h$ . In this example, in the case of cubic splines the  $L^2$  errors were of the same order of magnitude up to about  $k/h = 1/2$ , increased slowly for larger values of  $k/h$ , and the scheme became unstable for  $k/h \geq 3$ . For quadratic splines, the  $L^2$  errors preserved their order of magnitude up to  $k/h = 1$  and increased slowly afterwards until violent instability occurred when  $k/h \geq 8$ .

These numerical results, in addition to many other similar ones that we obtained by integrating with this scheme *cnoidal-wave* solutions of the Serre system and also ‘artificial’ solutions of the nonhomogeneous equations, and in addition to similar results of [29], confirm the good accuracy and stability of the scheme and give us confidence in using it to simulate properties of the solitary waves of the Serre equations in the sequel.

**3.1. Remarks on solitary waves.** Since the numerical experiments of the two following subsections will focus on properties of the solitary waves of the Serre equations, we make here some observations comparing them to the solitary waves of the ‘classical’ Boussinesq system (CB) and the Euler equations.

By (60) we have for the solitary wave of the Serre equations with speed  $c > 1$  that

$$\begin{aligned} \zeta(\xi) &= A_S \operatorname{sech}^2(K\xi), \quad \xi \in \mathbb{R}, \\ A_S &= c^2 - 1, \quad K = \sqrt{3A_S/4c^2}. \end{aligned} \tag{61}$$

(Note, incidentally, that the speed-amplitude relation,  $c = \sqrt{1 + A_S}$ , coincides with Scott-Russell’s empirical formula.) In the case of CB there exist no closed-form solutions for the solitary waves but one may easily prove, cf. [4], that the speed of the solitary wave of amplitude  $A_{CB}$  is given by the formula

$$c^2 = \frac{6(1 + A_{CB})^2}{3 + 2A_{CB}} \cdot \frac{(1 + A_{CB}) \ln(1 + A_{CB}) - A_{CB}}{A_{CB}^2}. \tag{62}$$

Letting

$$f(x) = \frac{6(1 + x)^2}{3 + 2x} \cdot \frac{(1 + x) \ln(1 + x) - x}{x^2} - 1, \quad x > 0,$$

one may see by straightforward calculus arguments that  $f$  is continuous on  $[0, \infty)$ ,  $f(0) = 0$ , and  $f$  is monotonically increasing on  $[0, \infty)$ . Moreover,  $f(x) < x$  for  $x > 0$ , from which we infer that for solitary waves of the CB and the Serre systems of the same speed  $c > 1$ , since  $A_S = c^2 - 1 = f(A_{CB})$ , it holds that

$$A_S < A_{CB}. \tag{63}$$

Since for  $x$  small we have  $f(x) = x - \frac{1}{6}x^2 + \frac{1}{90}x^3 + \frac{7}{240}x^4 + O(x^5)$ , inverting the series, we get for  $y = c^2 - 1$ ,  $c > 1$ ,  $y$  small, that

$$A_{CB} = y + \frac{1}{6}y^2 + \frac{2}{45}y^3 - \frac{13}{1080}y^4 + O(y^5). \tag{64}$$

The analog of the expansion of  $c^2 - 1$  in terms of the amplitude of the solitary wave of the Euler equations has been derived e.g. by Long, [26], equation (46). Inverting Long’s expansion we obtain for  $y = c^2 - 1$ ,  $c > 1$ ,  $y$  small,

$$A_{Euler} = y + \frac{1}{20}y^2 + \frac{67}{1400}y^3 + \frac{73}{1600}y^4 + O(y^5). \tag{65}$$

(To our knowledge, convergence of this expansion has not been proved.) Comparing (64) and (65) with the exact relation

$$A_S = y, \tag{66}$$

we see that for  $c$  close to 1  $A_S < A_{Euler} < A_{CB}$  and that  $|A_{Euler} - A_S| < |A_{Euler} - A_{CB}|$ . These observations are confirmed by Figure 1 in which the solitary waves for the Euler equations (computed by the numerical method of [14]) and the ‘classical’ Boussinesq system (computed by a spectral spatial discretization and the

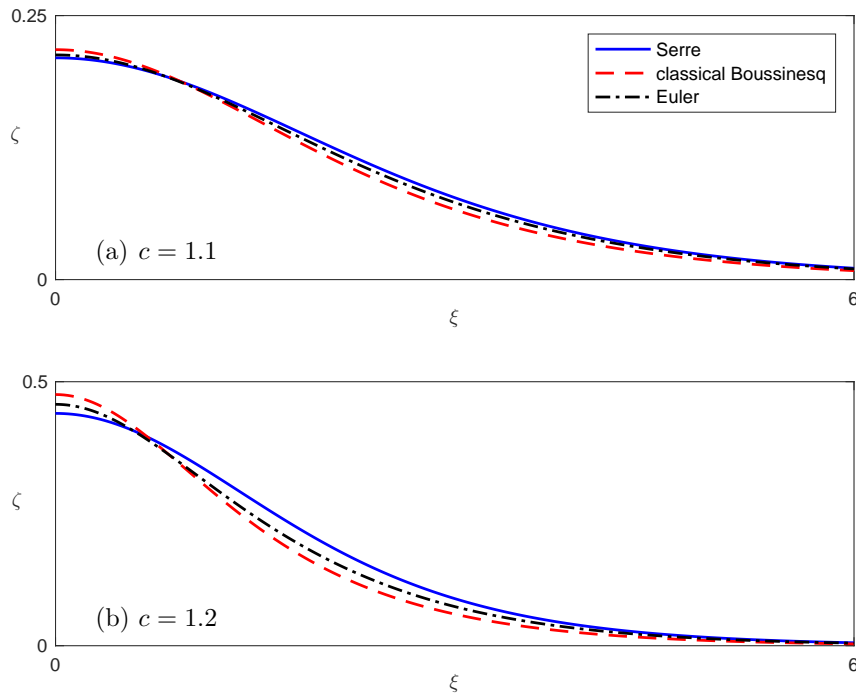


FIGURE 1. Profiles of solitary waves for  $\xi = x - ct$  (only the right-hand halves of the waves are shown) for the Serre, CB, and Euler equations, for speeds (a)  $c = 1.1$ , (b)  $c = 1.2$ .

Petviashvili nonlinear system solver as in [1]) are compared for  $c = 1.1$  and  $c = 1.2$  to the solitary waves of the Serre system. In Figure 1 the numerical values are

$$\begin{aligned} A_S = 0.21, \quad A_{Euler} = 0.21276, \quad A_{CB} = 0.21774 \quad \text{for } c = 1.1, \\ A_S = 0.44, \quad A_{Euler} = 0.45715, \quad A_{CB} = 0.47573 \quad \text{for } c = 1.2. \end{aligned}$$

Our numerical evidence agrees with the analogous results of Li *et al.*, [25], where a comparative study was made by numerical means of solitary waves of the Euler equations, the CB system, the KdV equation and the Serre equations (called the Su-Gardner equations). A general conclusion from [25] is that up to speeds (in the variables of the paper at hand) of about 1.2 the amplitude and mass, i.e. the integral  $\int \eta dx$ , of the Serre solitary wave, are closer to the analogous quantities of the solitary wave of the Euler equations than their CB counterparts. For larger speeds the solitary waves of both long-wave models are not accurate approximations of the solitary wave of the Euler equations.

**3.2. Resolution of initial profiles into solitary waves.** It is well known that solitary waves play a distinguished role in the evolution and long-time behavior of solutions of the initial-value problem for the associated nonlinear dispersive systems that emanate from initial data that decay suitably fast at infinity. This property, of the *resolution* of general initial data into sequences of solitary waves followed by slower oscillatory dispersive tails of small amplitude, has been rigorously proved for integrable one-way models such as the KdV equation and observed numerically in the case of many other examples of nonlinear dispersive wave equations that possess solitary waves. In particular, this property has been observed in the case of the Serre equations in numerical experiments in [25], [29], and [16].

In order to complement these studies we integrated the Serre system with our fully discrete scheme (using cubic splines for the spatial discretization) on the interval  $[-300, 300]$ , with  $h = 0.1$  and  $k = 0.01$ . We studied the evolution of initial Gaussian profiles of the form  $\zeta(x, 0) = ae^{-bx^2}$ ,  $u(x, 0) = 0$  (recall that  $\eta = 1 + \zeta$ ), and compared with the analogous evolution of solutions of the ‘classical’ Boussinesq system (CB) with the same initial conditions. The initial profile evolves, after some time, into two symmetric wavetrains that travel in opposite directions and consist of a number of solitary waves plus a trailing dispersive tail. (In

Figures 2-4 only the rightwards-travelling part of the solution is shown.) In Figure 2 one may observe the solution emanating from the Gaussian with  $a = 0.5$ ,  $b = 0.05$ ; by  $t = 200$  two solitary waves have been formed for both systems. Figures 3 and 4 show analogous resolution profiles produced by Gaussians with  $a = 1$ ,  $b = 0.05$ , and  $a = 5$ ,  $b = 0.2$ , at  $t = 200$  and  $t = 140$ , respectively. By these temporal values three solitary waves have emerged for both systems in both cases. (The magnified graph in Figure 4 shows the smallest generated solitary wave pulses of both systems and the base of the next larger solitary wave of the Serre system, and provides a clear view of the dispersive tails of the two wavetrains.) We observe that the emerging solitary waves of the Serre system have smaller speeds and amplitudes than their companion CB solitary waves. The oscillations of the dispersive tail behind the Serre solitary wavetrains are much larger in amplitude and number than those of the dispersive tail in the CB case, which is a nonlinear feature of the Serre system as the linearized equations of both systems coincide. It might be of interest to point out that we ran several experiments with Gaussian initial profiles varying the parameters  $a$  and  $b$ ; in each case we noted that the number of solitary waves  $N_s$  produced by about  $t = 200$  was the same for both systems. In particular, the results of Table 1 of [5] apparently hold for the Serre system as well and therefore  $N_s$  appears to be proportional to  $\int \sqrt{\eta_0 - 1} \sim (a/b)^{1/2}$  as in the case of the KdV equation, [34], and as predicted by asymptotic analysis for the Serre system in [16].

**3.3. Overtaking collisions of solitary waves.** As is well known, when two solitary waves of many non-linear dispersive systems collide, the solitary waves that emerge remain largely unchanged, having in general slightly different amplitudes and speeds and undergoing small phase shifts. With the exception of integrable equations, such as the KdV, the collisions are inelastic, producing in addition small-amplitude dispersive oscillatory tails after the interactions.

In the case of the Serre equations head-on collisions of solitary waves have appeared in the literature, cf. e.g. [29] and its references. In this section we shall focus on *overtaking collisions* of solitary waves of different speeds propagating in the same direction. The highly accurate numerical scheme tested in section 3.1 affords a detailed simulation of this type of interactions. Overtaking collisions for the Serre system have been previously studied numerically in [27], [25], [29]. For analogous studies in the case of Boussinesq systems cf. e.g. [5], [4]. A thorough study of collisions of solitary waves, and in particular of overtaking

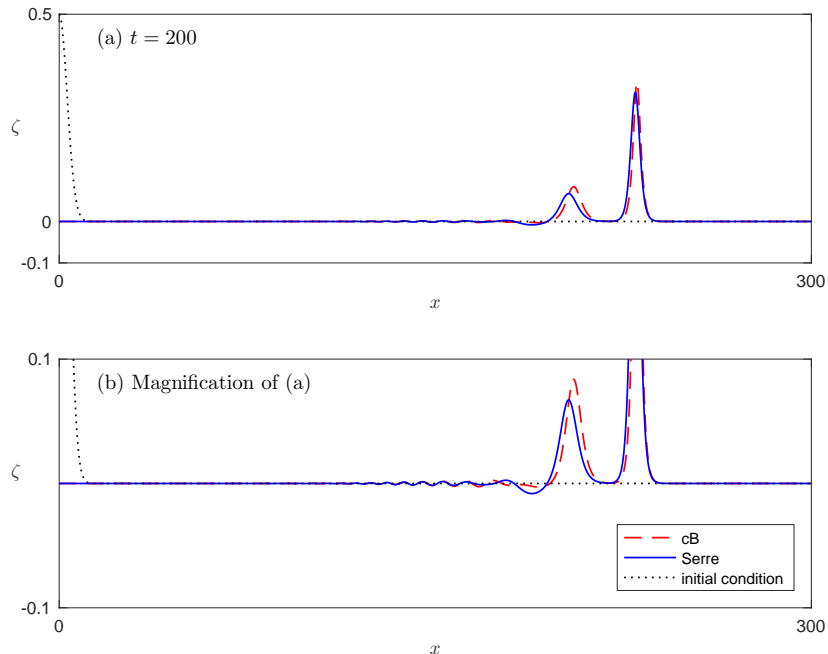


FIGURE 2. Resolution of a Gaussian into solitary waves ( $a = 0.5$ ,  $b = 0.05$ ), Serre and CB systems.

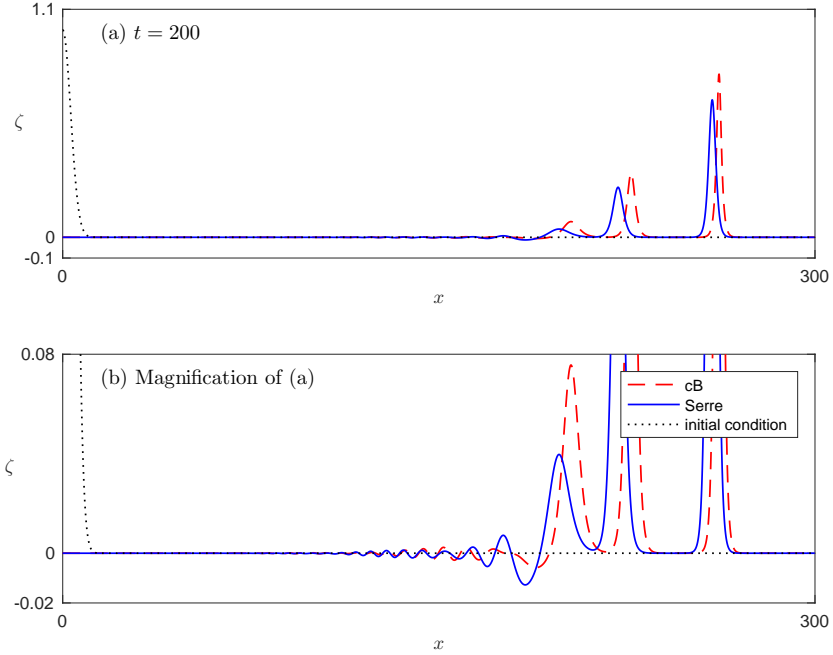


FIGURE 3. Resolution of a Gaussian into solitary waves ( $a = 1$ ,  $b = 0.05$ ), Serre and CB systems.

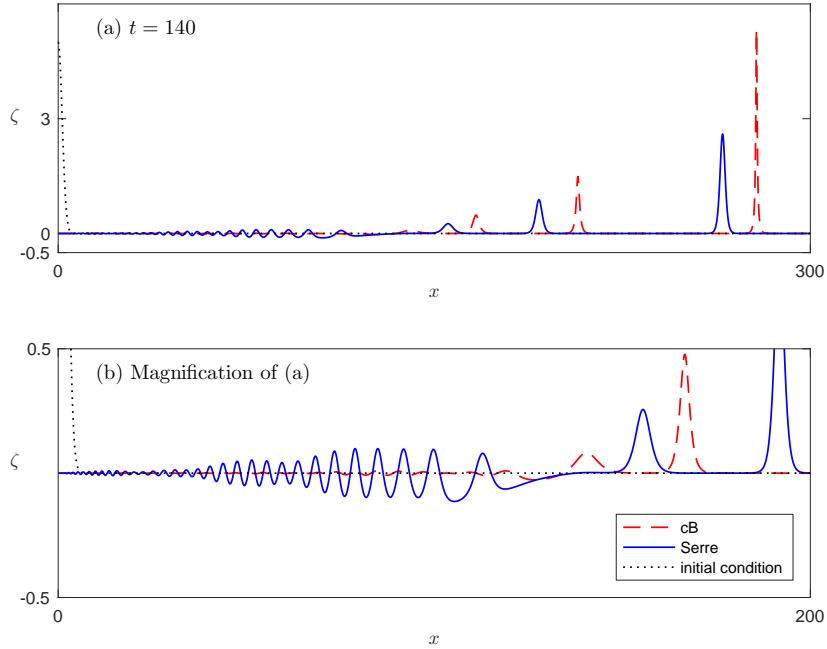


FIGURE 4. Resolution of a Gaussian into solitary waves ( $a = 5$ ,  $b = 0.2$ ), Serre and CB systems.

collisions, by numerical and experimental means has been performed by Craig *et al.* [12] in the case of the Euler equations.

We studied the overtaking collisions by integrating the Serre equations with our fully discrete method using cubic splines on the spatial interval  $[-400, 400]$  taking  $h = 0.1$  and  $k = 0.01$ . The initial conditions were two solitary waves of the form (60), of which the larger one, of amplitude  $A_S = a_1$ , was centered at



$x = -30$ , while the smaller, of amplitude  $a_2 < a_1$ , was centered at  $x = 30$ . In the sequel we let  $r = a_1/a_2$ , and, unless otherwise indicated, we took  $a_1 = 1$  and varied  $a_2$ .

For small values of  $r$ , specifically for  $r \leq 3.0967$ , we observed that during the collision the amplitude of the larger solitary wave decreases monotonically while that of the smaller one increases also monotonically. At the end of the interaction the two waves have exchanged the order of their positions and in place of the smaller there emerges a solitary wave closely resembling the larger one and vice versa. During this interaction two distinct maxima of the solution exist at all times. Therefore, this type of interaction is analogous to the overtaking collision of two solitons of the KdV equation classified by Lax in Lemma 2.3 of [22] as case (a). In Figure 5 we show an example of this type of collision with  $r = 2.5$ . The  $\zeta$ -profiles of the solution are depicted as functions of  $x$  at several temporal instances close to the interaction in Figure 5(i). In Figure 5(ii) we show the peak amplitudes of the two waves as functions of time. (In order to compute a peak amplitude with high accuracy at each  $t^n$ , we locate a node  $x_i$  where the fully discrete approximation  $\zeta(x, t^n)$  achieves a local discrete maximum, solve  $\zeta_x(x, t^n) = 0$  in the vicinity of  $x_i$  by Newton's method, and find the peak value and its location  $x^*$ . For  $r \leq 3.0967$  the code was able to find two distinct maxima for all  $t$ .) After the interaction the larger solitary wave suffers a slight loss of amplitude, while the smaller one gains a small amount. This is shown in the first line of Table 1, where the values 'a<sub>1</sub> after', 'a<sub>2</sub> after' are the stabilized

Lax case	$r$	$a_1$	$a_1$ after	$a_2$	$a_2$ after
(a)	2.5	1	0.99966	0.4	0.40051
(b)	3.125	1	0.99965	0.32	0.32065
(c)	5.0	1	0.99976	0.2	0.20066

TABLE 1. Amplitudes of the solitary waves before and after the interaction ( $a_1 =$  amplitude of the large s.w.,  $a_2 =$  amplitude of the small s.w.).

amplitudes of the large and small solitary wave, respectively, well after the interaction.

Figure 5(iii) shows the paths of the locations of the peaks  $x^*$  of the solitary waves in the  $x, t$ -plane. During the interaction the smaller (slower) solitary wave undergoes a backward phase shift while the larger (faster) wave is displaced forward by a smaller amount. (The phase shifts are measured relative to the positions of the peaks in the absence of interaction, indicated by the dotted lines in Fig 5(iii).) The absolute values of the phase shifts ( $\Delta x^*$ ) are recorded, at the indicated temporal values, in Table 2. For values of  $r \geq 3.9784$

Lax case	$r$	small s.w.	large s.w.	$t$
(a)	2.5	3.1	2.4	270
(b)	3.125	2.6	2.1	230
(c)	5.0	2.1	1.4	230

TABLE 2. Absolute values of phase shifts of the small and the large solitary waves measured at the indicated times.

(the values of  $r$  where a transition in type occurs have been determined to four decimals) the interaction resembles the one shown in Figure 6, which corresponds to  $r = 5$ . The large solitary wave covers the small one completely, for a while there is only one pulse visible, and finally the small solitary wave is re-emitted from the backside of the large one. Hence this type of interaction is analogous to that of case (c) of Lax's Lemma 2.3 for the KdV. As may be seen in Figures 6(ii) and (iii) the code was able to detect two distinct local maxima initially for  $t \leq 172.50$  and again for  $t \geq 192.47$ . The stabilized amplitudes after the interaction and the phase shifts at  $t = 230$  are given in Tables 1 and 2, respectively. They resemble qualitatively those of case (a).

In the range  $3.1088 \leq r \leq 3.9783$ , the interaction looks like the one shown in Figure 7, which corresponds to the value  $r = 3.125$ . Initially, the large solitary wave covers the small one and for a small temporal interval only one local maximum is observed. Subsequently, the smaller pulse reappears and grows in amplitude, while the amplitude of the larger one diminishes. (During this phase two distinct local maxima exist.) After the two amplitudes take momentarily equal values, the process is repeated in reverse: The two waves exchange positions, the small one is absorbed for a small temporal interval by the large one and is finally re-emitted as a separate small solitary wave from the backside of the larger one. Therefore this type of

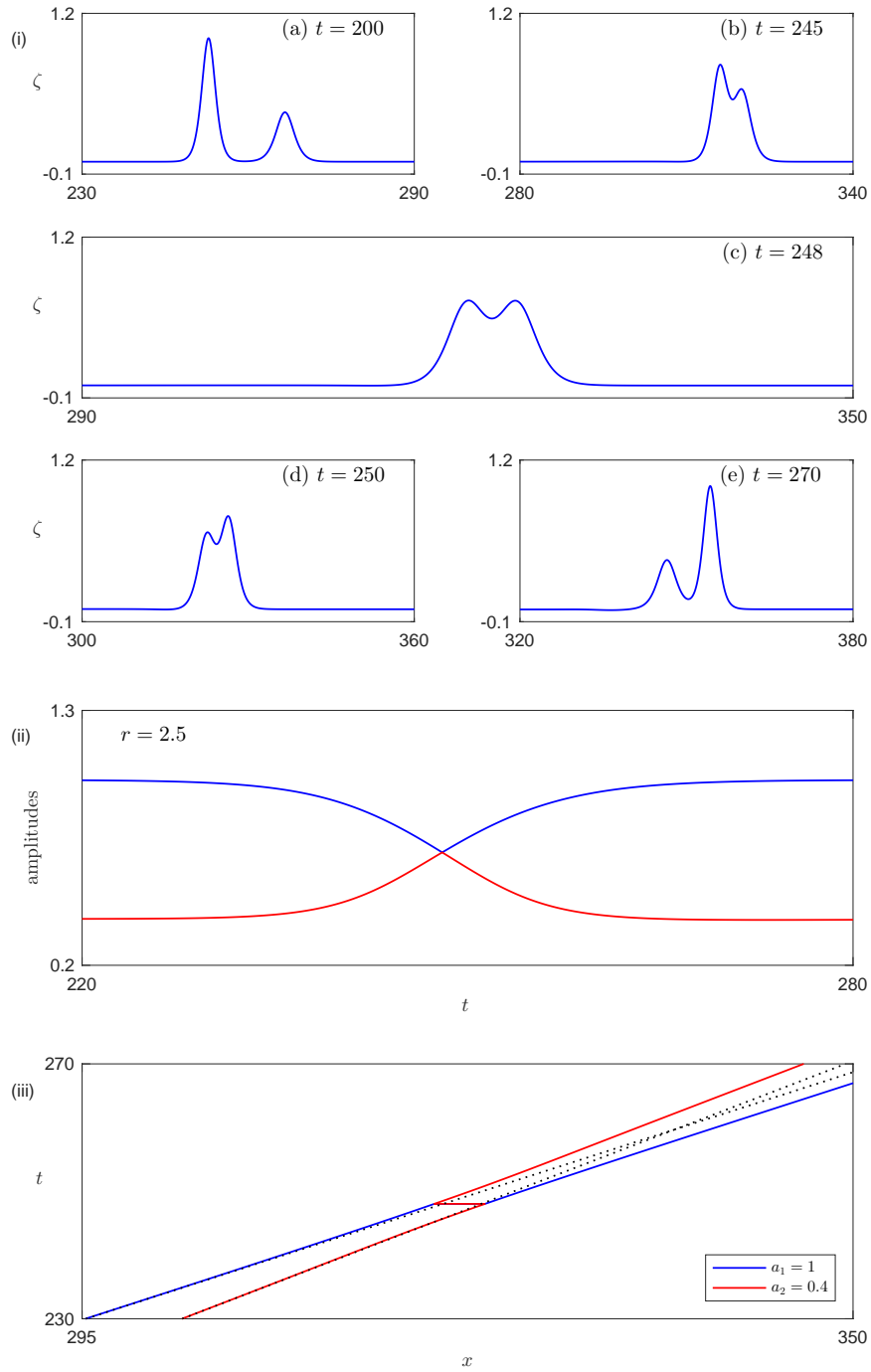


FIGURE 5. Overtaking collision,  $r = 2.5$  (Lax case (a)). (i):  $\zeta$ -profiles of the solution at various temporal instances, (ii): Peak amplitudes of  $\zeta$  as functions of  $t$ , (iii): Location of the peaks in the  $x,t$ -plane.

interaction, intermediate between the two previous types, is analogous to that of case (b) in Lax's lemma, valid for the KdV. The event may be observed more clearly in the evolution of the peak amplitudes shown in Fig. 7(ii). The code was able to detect two distinct local maxima up to  $t = 212.96$  and only one maximum for  $t \in [212.97, 214.35]$  when the smaller solitary wave is absorbed by the pursuing larger wave. Subsequently,

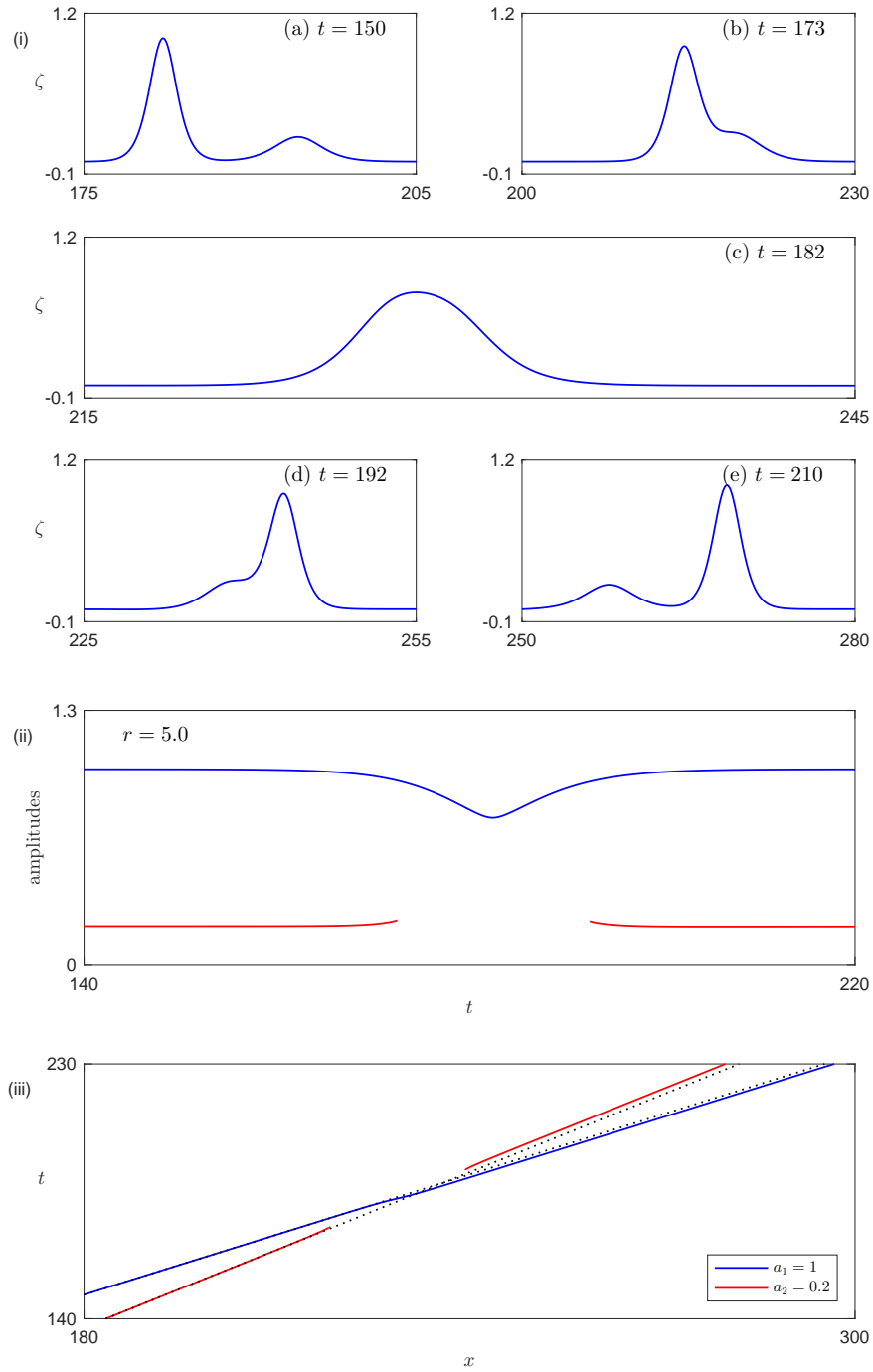


FIGURE 6. Overtaking collision,  $r = 5$  (Lax case (c)). (i):  $\zeta$ -profiles of the solution at various temporal instances, (ii): Peak amplitudes of  $\zeta$  as functions of  $t$ , (iii): Location of peaks in the  $x, t$ -plane.

two distinct peaks are recorded again until  $t = 219.95$  when the smaller wave is absorbed again by the larger one. The code was not able to detect a second peak for  $t \in [219.96, 221.84]$ . After this temporal interval two local maxima reappeared. The quantitative scattering data for this interaction (amplitudes and phase shifts)

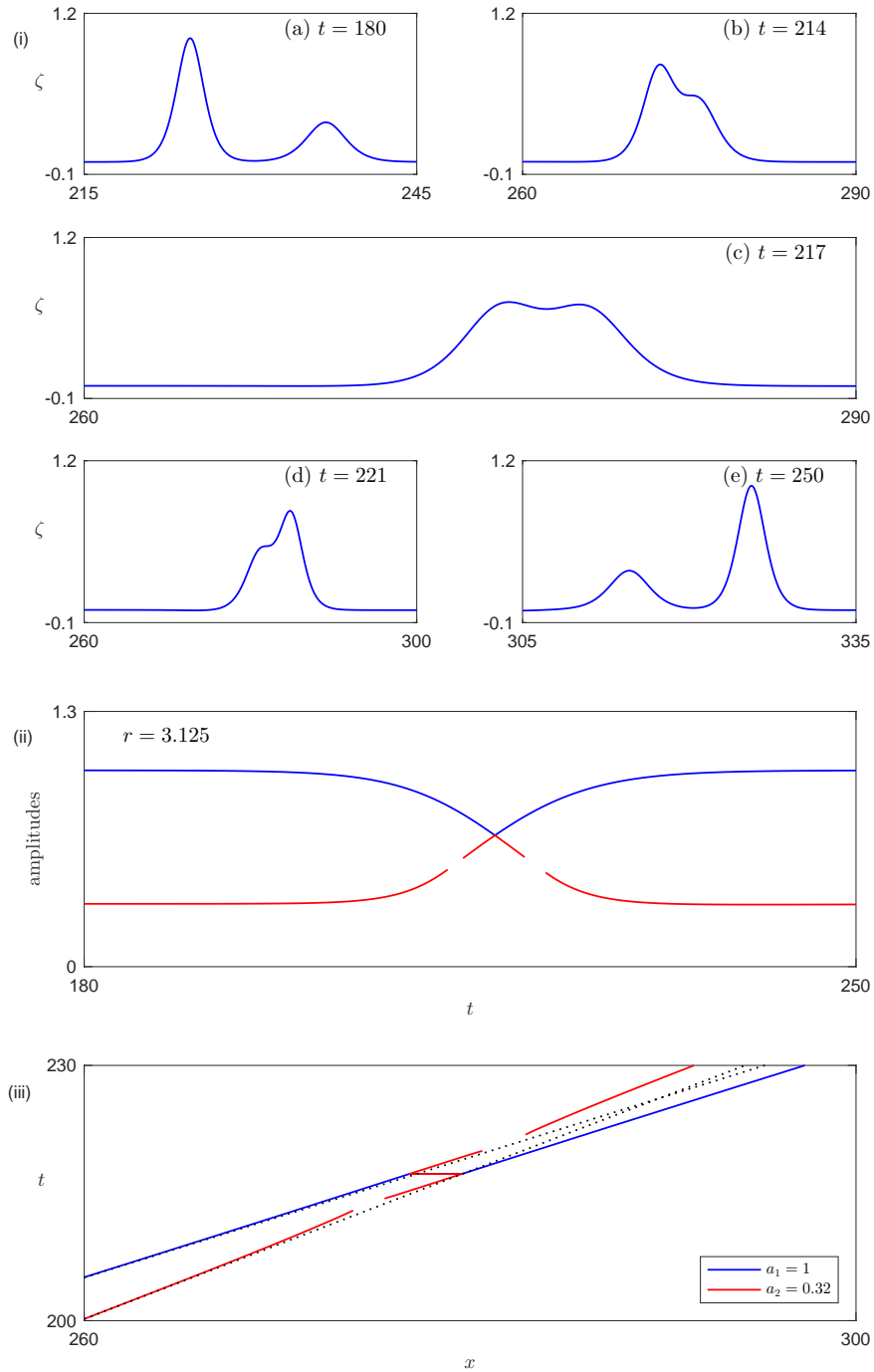


FIGURE 7. Overtaking collision,  $r = 3.125$  (Lax case (b)). (i):  $\zeta$ -profiles of the solution at various temporal instances, (ii): Peak amplitudes of  $\zeta$  as function of  $t$ , (iii): Location of the peaks in the  $x,t$ -plane.

are given in the middle lines of Tables 1 and 2, respectively; they resemble qualitatively the corresponding values of cases (a) and (c).

It should be noted that whereas the signs of the phase shifts of the emerging solitary waves (the larger wave is pushed forward while the smaller one is delayed) are the same as the ones observed in the case of

the Euler equations in [12] (and also in the case of the CB, [4]), Table 1 shows that in all cases after the interaction the larger wave diminishes slightly in amplitude while similar to the Serre case.)

As in the case of the Boussinesq systems and of the Euler equations, the interaction is *inelastic*. In all cases we observed that after the interaction two kinds of dispersive small-amplitude residuals were generated: A dispersive tail of small-wavelength, decaying in amplitude oscillations that travel to the right trailing the solitary waves, and a single  $N$ -shaped, small-amplitude wavelet of large wavelength that travels to the left. These are illustrated in Figure 8 that shows the  $\zeta$ -profile of the solution in the case  $r = 3.125$  at  $t = 450$  and its magnification in the direction of the  $\zeta$ -axis. (The solution has been translated periodically so that the solitary waves and the residuals appear near the center of the figure.) The dispersive tail and the wavelet are of  $O(10^{-3})$  in amplitude. This structure of the residual was qualitatively the same for all values of  $r$  that we tried in the various Lax cases. It should be noted that it resembles the residual of overtaking collisions observed in the case of various Boussinesq systems, [5], [4], but perhaps not the residual appearing in numerical simulations of similar interactions in the case of the Euler equations; cf. e.g. Figure 19 of [12], where only the wavelet seems to have been produced.

Let us also point out that the intervals of  $r$  in which the overtaking collisions resemble those of the Lax cases (a), (b), and (c) depend on the value of, say,  $a_1$  as well, i.e. the type of interaction does not depend solely on  $r$  as in the case of KdV. For example, when we took  $a_1 = 1.5$ , we found that the interactions were of type (a) for  $r = a_1/a_2$  less than 3.372, of type (c) for  $r > 4.545$ , and of type (b) for values of  $r$  in between. This is akin to what was observed for the Euler equations in [12]. As one final note of interest, one may observe that the temporal intervals [212.97,214.35] and [219.96, 221.84], during which there is apparently only one peak in the interaction of type (b) shown in Figure 7(ii) in the case  $a_1 = 1$ ,  $r = 3.125$ , are of unequal duration, the first one being smaller than the second. This led us to investigate whether these could be values of  $r$  for which the first interval disappears but the second does not. We found that for  $3.0968 \leq r \leq 3.1087$  this was indeed the case, illustrated for  $r = 3.1056$  in the first one being smaller than the second. This led us to investigate whether these could be values of  $r$  for which the first interval disappears but the second does not. We found that for  $3.0968 \leq r \leq 3.1087$  this was indeed the case, illustrated for  $r = 3.1056$  in Figure 9. In this type of interaction initially there are apparently two distinct local maxima that exchange heights and then the smaller peak is absorbed by the larger one to reemerge later at the back of the large

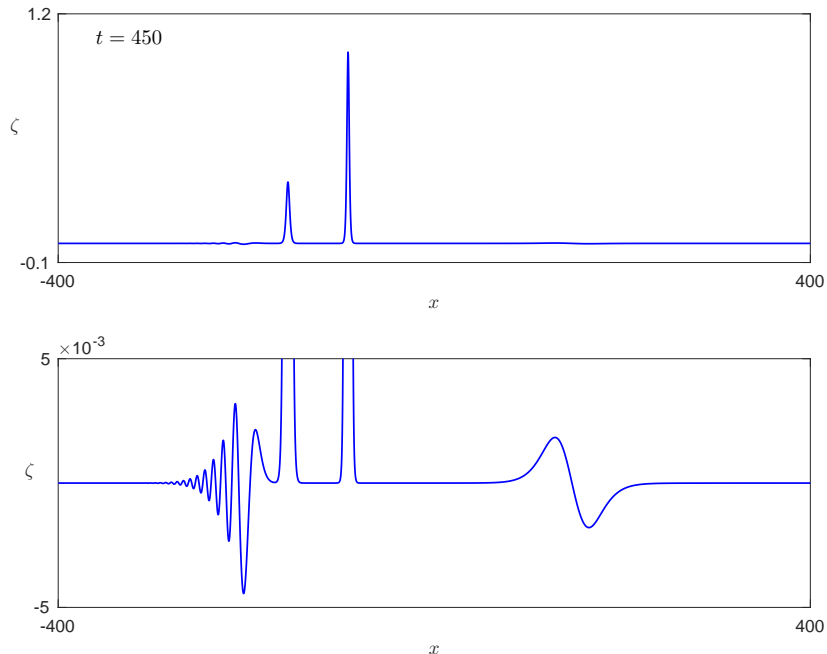


FIGURE 8. The dispersive tail and the wavelet in the case  $r = 3.125$ .

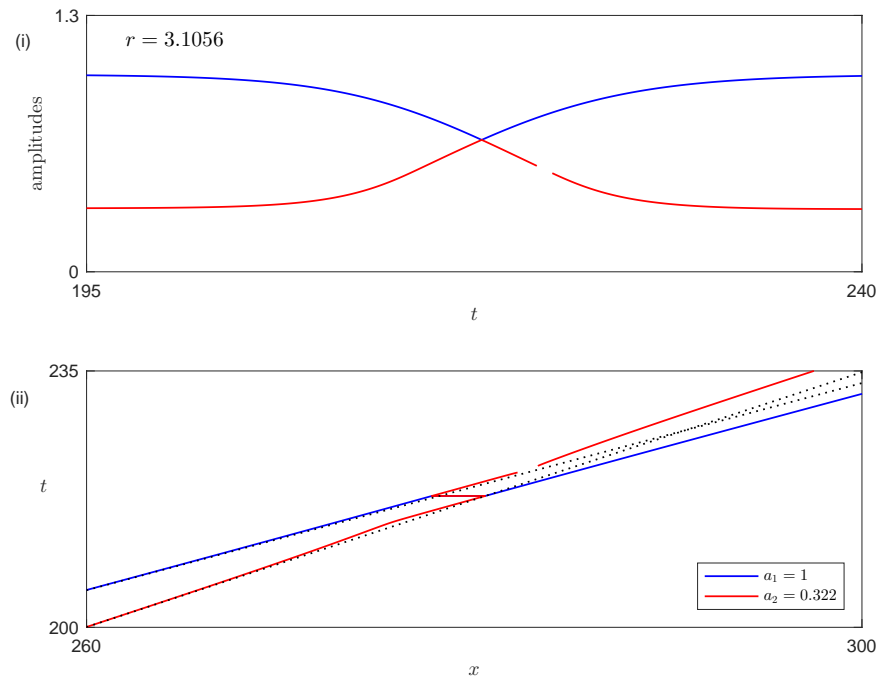


FIGURE 9. (i): Peak amplitudes of  $\zeta$  as functions of  $t$ , (ii): Locations of the peaks in the  $x,t$ -plane. Intermediate case between (a) and (b),  $r = 3.1056$ .

wave. Thus this interaction appears to be of an intermediate (transitional) type between cases (a) and (b) and we label it accordingly as case (ab).

In conclusion, Table 3 shows the intervals of  $r$  (for  $a_1 = 1$ ) and the corresponding type of interaction that we observed. In the case (a) our code was always able to find two distinct local maxima. In the transitional

Cases	(a)	transitional (ab)	(b)	(c)
$r$	$(1, 3.0967]$	$[3.0968, 3.1087]$	$[3.1088, 3.9783]$	$[3.9784, +\infty)$

TABLE 3. Overtaking collisions, Serre equations,  $a_1 = 1$ ,  $r = a_1/a_2$ . Lax cases and corresponding intervals of  $r$ .

case (ab) there was only one temporal interval in which a unique local maximum was found, while in case (b) two such disjoint intervals were detected. These two intervals merge into a single larger interval in case (c).

## REFERENCES

- [1] J. ALVAREZ AND A. DURAN, *Petviashvili type methods for traveling wave computations : II Acceleration with vector extrapolation methods*, Math. and Computers in Simulation, 123 (2016), pp. 19–36.
- [2] D. C. ANTONOPOULOS AND V. A. DOUGALIS, *Error estimates for the standard Galerkin finite element method for the Shallow Water equations*, Math. Comp., 85 (2016), pp. 1143–1182.
- [3] D. C. ANTONOPOULOS AND V. A. DOUGALIS, *Error estimates for Galerkin approximations of the ‘classical’ Boussinesq system*, Math. Comp., 82 (2013), pp. 689–717.
- [4] D. C. ANTONOPOULOS AND V. A. DOUGALIS, *Numerical solution of the ‘classical’ Boussinesq system*, Math. and Computers in Simulation, 82 (2012), pp. 984–1007.
- [5] D. C. ANTONOPOULOS, V. A. DOUGALIS, AND D. E. MITSOTAKIS, *Numerical solution of Boussinesq systems of the Bona-Smith family*, Appl. Numer. Math., 60 (2010), pp. 314–336.
- [6] D. C. ANTONOPOULOS, V. A. DOUGALIS, AND D. E. MITSOTAKIS, *Galerkin approximations of periodic solutions of Boussinesq systems*, Bull. Greek. Math. Soc., 57 (2010), pp. 13–30.
- [7] E. BARTHÉLEMY, *Nonlinear shallow water theories for coastal waves*, Surv.Geophys., 25 (2004), pp. 315–337.

- [8] P. BONNETON, E. BARTHÉLEMY, F. CHAZEL, R. CIENFUEGOS, D. LANNES, F. MARCHE, AND M. TISSIER, *Recent advances in Serre-Green Naghdi modelling for wave transformation, breaking and runup processes*, Eur. J. Mech. B/Fluids, 30 (2011), pp. 635–641.
- [9] P. BONNETON, F. CHAZEL, D. LANNES, F. MARCHE, AND M. TISSIER, *A splitting approach for the fully nonlinear and weakly dispersive Green-Naghdi model*, J. Comp. Phys., 230 (2011), pp. 1479–1498.
- [10] J. S. ANTUNES DO CARMO, *Applications of Serre and Boussinesq type models with improved linear dispersion characteristics*, Proc. Congress on Num. Methods in Eng'g, 25–28 June 2013, Bilbao, SEMNI 2013.
- [11] J. D. CARTER AND R. CIENFUEGOS, *The kinematics and stability of solitary and cnoidal wave solutions of the Serre equations*, Eur. J. Mech. B/Fluids, 30 (2011), pp. 259–268.
- [12] W. CRAIG, P. GUYENNE, J. HAMMACK, D. HENDERSON, AND C. SULEM, *Solitary water wave interactions*, Phys. Fluids, 18 (2006), pp.057106, 1–25.
- [13] V. A. DOUGALIS AND O. A. KARAKASHIAN, *On some high-order accurate fully discrete Galerkin methods for the Korteweg-de Vries equation*, Math. Comp., 45 (1985), pp. 329–345.
- [14] D. DUTYKH AND D. CLAMOND, *Efficient computation of steady solitary gravity waves*, Wave Motion, 51 (2014), pp. 86–99.
- [15] D. DUTYKH, D. CLAMOND, P. MILEWSKI, AND D. MITSOTAKIS, *Finite volume and pseudo-spectral schemes for the fully nonlinear 1D Serre equations*, European J. Appl. Math., 24 (2013), pp. 761–787.
- [16] G. A. EL, R. H. J. GRIMSHAW AND N. F. SMYTH, *Asymptotic description of solitary wave trains in fully nonlinear shallow-water theory*, Physica D, 237 (2008), pp. 2423–2435.
- [17] A. E. GREEN, N. LAWS, AND P. M. NAGHDI, *On the theory of water waves*, Proc. R. Soc. London A, 338 (1974), pp. 43–55.
- [18] A. E. GREEN AND P. M. NAGHDI, *A derivation of equations for wave propagation in water of variable depth*, J. Fluid Mech., 78 (1976), pp. 237–246.
- [19] S. ISRAWI, *Large time existence for 1D Green-Naghdi equations*, Nonlinear Anal. Theory Methods Appl., 74 (2011), pp. 81–93.
- [20] D. LANNES, *The Water Waves Problem: Mathematical Analysis and Asymptotics*, American Mathematical Society, Providence, R. I., 2013.
- [21] D. LANNES AND P. BONNETON, *Derivation of asymptotic two-dimensional time-dependent equations for surface water propagation*, Phys. Fluids, 21 (2009), 016601.
- [22] P. D. LAX, *Integrals of nonlinear equations of evolution and solitary waves*, Comm. Pure Appl. Math., 21 (1968), pp. 467–490.
- [23] Y. A. LI, *Hamiltonian structure and linear stability of solitary waves of the Green-Naghdi equations*, J. Nonlinear Math. Phys., 9 (2002), pp. 99–105.
- [24] Y. A. LI, *A shallow-water approximation of the full water wave problem*, Comm. Pure Appl. Math., 59 (2006), pp. 1225–1285.
- [25] Y. A. LI, J. M. HYMAN, AND W. CHOI, *A numerical study of the exact evolution equations for surface waves in water of finite depth*, Stud. Appl. Math., 113 (2004), pp. 303–324.
- [26] R. R. LONG, *Solitary waves in the one-and two-fluid systems*, Tellus, 8 (1956), pp. 460–471.
- [27] R. M. MIRIE AND C. H. SU, *Collision between two solitary waves. Part 2. A numerical study*, J. Fluid Mech., 115 (1982), pp. 475–492.
- [28] D. MITSOTAKIS, D. DUTYKH, AND J. D. CARTER, *On the nonlinear dynamics of the traveling-wave solutions of the Serre equations*, *arXiv:1404.6725* (To appear in Wave Motion).
- [29] D. MITSOTAKIS, B. ILAN, AND D. DUTYKH, *On the Galerkin/finite element method for the Serre equations*, J. Sci. Comput., 61 (2014), pp. 166–195.
- [30] F. SERRE, *Contribution à l'étude des écoulements permanents et variables dans des canaux*, La Houille Blanche, 3 (1953), pp. 374–388, and pp. 830–872.
- [31] C. H. SU AND C. S. GARDNER, *Korteweg-de Vries equation and generalizations. III. Derivation of the Korteweg-de Vries equation and Burgers equation*, J. Math. Phys., 10 (1969), pp. 536–539.
- [32] F.J.SEABRA-SANTOS, D.P.RENOUARD, AND A.M.TEMPERVILLE, *Numerical and experimental study of a transformation of a solitary wave over a shelf or isolated obstacle*, J.Fluid.Mech., 176 (1987), pp. 117–134.
- [33] V. THOMÉE AND B. WENDROFF, *Convergence estimates for Galerkin methods for variable coefficient initial value problems*, SIAM J. Numer. Anal., 11 (1974), pp. 1039–1068.
- [34] G. B. WHITHAM, *Linear and Nonlinear Waves*, Wiley, New York, 1974.

MATHEMATICS DEPARTMENT, NATIONAL AND KAPODISTRIAN UNIVERSITY OF ATHENS, 15784 ZOGRAPHOU, GREECE AND INSTITUTE OF APPLIED AND COMPUTATIONAL MATHEMATICS, FORTH, 70013 HERAKLION, GREECE  
*E-mail address:* antonod@math.uoa.gr

MATHEMATICS DEPARTMENT, NATIONAL AND KAPODISTRIAN UNIVERSITY OF ATHENS, 15784 ZOGRAPHOU, GREECE AND INSTITUTE OF APPLIED AND COMPUTATIONAL MATHEMATICS, FORTH, 70013 HERAKLION, GREECE  
*E-mail address:* doug@math.uoa.gr

VICTORIA UNIVERSITY OF WELLINGTON, SCHOOL OF MATHEMATICS AND STATISTICS, WELLINGTON 6140, NEW ZEALAND  
*E-mail address:* dimitrios.mitsotakis@vuw.ac.nz  
*URL:* <http://dmitsot.googlepages.com/>